SEA TO DIGITAL REALITY

COMPARATIVE ANALYSIS OF UNDERWATER STRUCTURE FROM MOTION PHOTOGRAMMETRY PLATFORMS AND THEIR INTEGRATION INTO AN IMMERSIVE AUGMENTED REALITY APPLICATION

A THESIS SUBMITTED TO THE GRADUATE DIVISON OF THE UNIVERSITY OF HAWAIʻI AT HILO IN PARTIAL FULFILLMENT OF THE REQUIREMENTS FOR THE DEGREE OF

MASTER OF SCIENCE

IN

TROPICAL CONSERVATION BIOLOGY AND ENVIRONMENTAL SCIENCE

AUGUST 2023

BY

ALEXANDER J. SPENGLER

THESIS COMMITTEE:

JOHN HR BURNS

GRADY WEYENBERG

DREW GRAY

KEYWORDS: UNDERWATER PHOTOGRAMMETRY, CORAL REEF, 3D RECONSTRUCTION, ACTION CAMERA, AUGMENTED REALITY, SCIENCE COMMUNICATION

ACKNOWLEDGEMENTS

I extend my heartfelt gratitude to numerous individuals who have played a crucial role in shaping this project:

Firstly, I am deeply grateful to my esteemed thesis committee, comprised of Dr. John Burns, Dr. Grady Weyenberg, and Dr. Drew Gray, whose invaluable guidance has been instrumental throughout this endeavor.

Additionally, I want to express my appreciation to Dr. Tracy Wiegner and Dr. Rebecca Ostertag, whose unwavering support and guidance during my time in the TCBES program have been invaluable.

My gratitude also extends to Kailey Pascoe and Sofi Ferreira, whose mentorship and guidance within the MEGA Lab have been pivotal to my growth and development.

Furthermore, I am indebted to the invaluable contributions of John Graves, Dylan Kelling, Jared Khan, and Kim Yumul, who played an essential role in collecting the data for this project.

Lastly, my sincere thanks go to Keilani Bonis-Ericksen, Jazmin Heltzer, Jacob Wessling, Jordan Hemmerly, Alexa Runyan, Mia Lamirand, Shane Murphy, Dani Wilde, Carson Green, Olivia Jarvis, and Dawn McSwain for their generous assistance in thoroughly testing and debugging my mobile app.

To all these individuals, my deepest appreciation for your support and guidance throughout this journey.

ABSTRACT

Underwater 3D reconstruction tools play an important role in advancing the study and preservation of coral reef environments. This study assessed the viability of small action cameras, such as the GoPro Hero4, to serve as a comparable image collection platform to entry level DSLRs like the Canon 60D. The sensor and optical characteristics of a given camera system influence the accuracy and quality of 3D reconstructions. Examining the performance characteristics of action cameras is critical for assessing if these cheaper and simpler platforms can produce comparable data to the larger DSLR systems. . The findings from this study indicate that the GoPro Hero4 falls short in several key aspects compared to the Canon 60D, challenging its potential as a viable alternative. The Canon 60D's larger sensor size and lens allow for higher resolution and visually rich images, both of which are essential for accurate 3D reconstructions. The GoPro Hero4's small sensor and short lens introduce chromatic aberration, distortion, overexposure, and color accuracy issues which compromise the quality and precision of resulting 3D models. These limitations, along with disparities in quantitative metrics, highlight the challenges associated with using action cameras as DSLR replacements. However, for research objectives that are less dependent on fine detail, such as habitat structure metrics, small action cameras may offer comparable performance to established platforms like DSLRs. Identifying the performance thresholds of camera systems can provide useful information for scientists and organizations planning to integrate 3D reconstruction techniques into their research and monitoring of coral reefs.

This study also introduces an augmented reality (AR) application that allows users to explore and learn about underwater coral reefs and historical shipwrecks in the Pacific Ocean. The application leverages underwater photogrammetry data captured during scientific expeditions to create accurate 3D models of these environments. The Unity game engine and Vuforia AR engine are used to develop an interactive and immersive application. The AR app not only provides virtual access to these underwater environments but also incorporates educational content, interactive annotations, and informative overlays to enhance the user experience. The study also discusses the methods used for data acquisition and photogrammetry, application development, and publishing. The effectiveness of the AR application is evaluated through user feedback and performance testing. The app has been well-received, with positive ratings and downloads on both iOS and Android platforms. The study concludes that the app has

successfully bridged the gap between scientific data and the general public, fostering engagement, experiential learning, and environmental awareness. Future improvements could focus on expanding the number of targets and reducing the app's file size to enhance user engagement and accessibility.

TABLE OF CONTENTS

LIST OF FIGURES

LIST OF ABBREVIATIONS

2D ..... Two-Dimensional
3D ..... Three-Dimensional
DEM ..... Digital Elevation Model
GSD ..... Ground Sampling Distance
SfM ..... Structure from Motion
DSLR ..... Digital Single-lens Reflex
ISO ..... International Standards Organization
VRM ..... Vector Ruggedness Metric
GCP ..... Ground Control Point
SCUBA ..... Self-Contained Underwater Breathing Apparatus
M3C2 ..... Multiscale Model-to-model Cloud Comparison
SNR ..... Signal to Noise Ratio
AR ..... Augmented Reality
UI ..... User Interface
SLAM ..... Simultaneous Localization and Mapping
AAB ..... Android App Bundle
SDK ..... Software Development Kit
App ..... Application
GB ..... Gigabyte
MB ..... Megabyte

CHAPTER 1
COMPARATIVE ANALYSIS OF UNDERWATER PHOTOGRAMMETRY PERFORMANCE BETWEEN ESTABLISHED AND EMERGING CAMERA PLATFORMS

INTRODUCTION

Underwater ecosystems are complex and difficult to study due to the challenges of data collection in this dynamic and inaccessible environment. Over the past decade, new technologies have emerged to help capture the structural complexity and ecological characteristics of reefs at various scales (Roach et al. 2021). These tools have enabled ecologists to better understand and quantify ecosystem processes, including the relationships between structural complexity and biodiversity. Scientists have demonstrated that structural complexity drives biodiversity using a variety of methods in studies spanning decades (Roach et al. 2021). In tropical nearshore waters, the carbonate skeletons of stony corals make up the ecological foundation of the ecosystem and food web (Young et al. 2017). Coral skeletons create complex 3D habitats which facilitate high species diversity through the addition of habitable space (Risk 1972; Graham & Nash 2012; Fukunaga et al. 2020). High values of 3D structural complexity in coral reefs allows them to be some of the most species-dense habitats in the world's oceans (Reaka-Kudla 1997). Coral reefs provide spawning grounds and are interlinked with fisheries productivity which support coastal economies around the world (Hoegh-Guldberg et al. 2007). Reef complexity also plays a key role in providing important environmental services to humans, including enhancing coastal protection through the dissipation of wave energy transmitted over reefs (Cinner et al. 2012). Anthropogenic stressors, such as climate change, run-off, and overfishing, are major contributors to the decline in coral reefs across the globe (Hughes et al. 2003; Holbrook et al. 2015). This has led to the loss of more than half of all coral reefs throughout the world's oceans (Wilkinson & Souter 2008). Understanding the relationship between structural complexity and ecosystem processes is critical to effective ecosystem management and conservation efforts. As such, the continued development and application of new technologies and research methods will be crucial for advancing our understanding of these complex and valuable systems. Thus, finding efficient and affordable tools that produce quality data can help advance our ability to study and conserve coral reefs at a global scale. These tools can overcome the challenges of implementing 3D techniques, making them essential for understanding and monitoring these changing ecosystems.

Underwater photogrammetry is becoming increasingly utilized among marine scientists around the globe , particularly in fields such as archaeology and marine ecology, due to its flexibility, relatively low cost, and ease of use (Nocerino et al. 2019). Smaller and more affordable camera technologies have allowed for the implementation of digital cameras as a means to create high-accuracy 3D reconstructions of the marine benthos using photogrammetry tools (Burns et al. 2015). Divers can collect multiple overlapping images of underwater benthic habitats by swimming over an area of interest in a zig-zag pattern that supports optimal image overlap (70-80%). The area is then digitally reconstructed in 3D using those 2D images or video. This technology allows scientists and non-scientists alike to quickly capture quantifiable data (e.g., benthic cover, 3D complexity metrics) in environments where survey time is often restricted. Due to their popularity, low cost, and simplicity of use, action cameras have become an

accessible choice for SfM data collection and appeal to a broader user group of scientists and conservationists . Action camera based SfM surveys are a promising method for citizen science projects where data quality and overall effectiveness depend on standardization of sampling effort, bias minimization, participant engagement, and ease of training (Roach et al. 2021). The digital 3D reconstructions generated through SfM allow researchers to quantify structural habitat metrics and integrate them with ecological parameters to better understand complex relationships among reef organisms. (Ferreira et al. 2023). The development of low-cost, user-friendly, and accessible technologies for underwater photogrammetry and remote sensing has enabled a wider audience to engage with the study and monitoring of coral reef ecosystems (Raoult et al. 2016; Licuanan, Mordeno & Go 2021; Roberts et al. 2022).

Researchers assess the quality of 3D reconstructions using several metrics. Scale bars used during the data collection allow model correction based on the disconnect between the reconstructed 3D model and the source imagery (Dai, Feng, & Hough 2014). Deviations in measurement values between the reconstruction and source imagery produce a spatial error in terms of meters (Agisoft 2021). For a given model this value is the root mean square error in meters for all the scale bars in the model. Similarly, reprojection error is another useful indicator of the quality of the 3D reconstruction (Sapirstein 2016). Reprojection error measures the discrepancy between the projected positions of 3D points onto 2D image planes and the actual positions of corresponding feature points in the images. For a given 3D model, this value is the root mean square reprojection error average over all tie points on all images. Ground sampling distance (GSD) refers to the distance on the ground represented by a single pixel in an image. It quantifies the physical size of each pixel in real-world units. A smaller GSD value indicates a higher level of detail and finer spatial resolution, as each pixel represents a smaller area on the ground. Tie points are a concept commonly used in photogrammetry and refer to corresponding points identified in multiple images of the same scene or object. The quality and quantity of tie points play a significant role in the accuracy and reliability of the 3D reconstruction. More tie points and well-distributed correspondences across the images lead to a better alignment and more precise reconstruction. The image alignment step is a foundational component of the 3D reconstruction process and directly influences the density and accuracy of the resulting 3D point cloud . The point cloud is generated through a process of matching and correlating image features from multiple photos to estimate the 3D coordinates of corresponding points in the scene. The point cloud represents the surface geometry, and the number of points per area in the cloud can serve as a measure of detail in the final 3D model. Once the point cloud is generated, surfaces are formed by connecting the points using triangles or other polygonal faces. Mesh faces are essential in defining the surface topology and enabling the representation of 3D objects. More faces per area result in a more spatially accurate and realistic looking 3D model. In conclusion, the assessment of 3D reconstructions relies on various metrics such as scale bars, reprojection error, ground sampling distance, and the quantity and quality of tie points. These metrics play a crucial role in

determining the accuracy and level of detail in the final 3D model. By understanding and optimizing these factors, researchers can enhance the reliability and realism of 3D reconstructions, thereby advancing the application of photogrammetry and ensuring more accurate representations of the captured environments or objects.

In marine reef environments, researchers utilize SfM photogrammetry to produce high resolution 3D reconstructions of benthic habitats to ecologically characterize the systems. . Quantifying structural habitat characteristics, spatial distribution, and community composition of benthic organisms is crucial for understanding ecological function in these valuable marine ecosystems (Lecours et al. 2016; Fukunaga et al. 2019; Fukunaga et al. 2020; Fukunaga & Burns 2020). Several 3D habitat complexity metrics have been shown to successfully describe structural characteristics and model diversity and biomass of reef associated organisms (Fukunaga et al. 2020; Fukunaga & Burns 2020, Pascoe et al. 2021). Slope is measured in 3x3 cell windows and calculates the change in elevation for each cell in relation to its neighbor within the digital elevation model (DEM). This can give researchers insight into areas of variable relief and gradients. Vector ruggedness measure (VRM) quantifies the roughness or variability of the topography surface within a specific area. VRM is calculated based on the elevation values of neighboring cells in a DEM. VRM provides information about the spatial heterogeneity and complexity of the land surface. Higher VRM values indicate more rugged or uneven topography, while lower VRM values represent smoother or more uniform topography. Curvature refers to the rate of change in slope or the curvature of the surface at each point in a DEM. In this study I compute profile curvature. It provides information about the shape, concavity, and convexity of the topography. Surface Complexity refers to the level of intricacy and variability present in the surface as represented by the DEM data. It quantifies the spatial patterns and structures of the topography, considering factors such as elevation changes, slope variations, and other geometric attributes.

Understanding the relationship between the camera platform and accuracy of corresponding photogrammetrically derived 3D models is important for scientists and non-scientists alike. With decreasing coral cover and shifts in species composition, , there's a necessity to capture these changes in the most efficient way possible (Bellwood et al. 2019). Affordable action cameras are widely utilized in marine environments in a recreational capacity and the thorough evaluation of their scientific viability would lay the groundwork for their implementation in both professional research and citizen science settings. This study aims to provide a comparative analysis of underwater camera platforms commonly used in reef ecosystem data collection through a comprehensive breakdown of performance differences in the photogrammetry metrics between established platforms such as DSLRs and emerging alternatives such as action cameras. This work expands on well-established DSLR based underwater photogrammetry methods and directly applies those techniques to action cameras in the same environment. To address knowledge gaps related to the performance of underwater action camera

derived SfM photogrammetry, I directly compared 3D model quality metrics, 3D habitat structure metrics, and investigated how those metrics changed between both camera platforms with images collected at varying distances from the substrate. This research contributes to a better understanding of the potential of action cameras for capturing valuable data in underwater environments, opening new avenues for cost-effective and accessible data collection methods that can benefit marine research and conservation efforts.

HYPOTHESES

GENERAL HYPOTHESES

H1: There will be significant differences in 3D model accuracy and quality between the action camera and DSLR camera systems.

H2: There will be significant differences in 3D habitat complexity metrics between the action camera and DSLR camera systems.

H3: There will be significant differences in 3D model accuracy, quality, and 3D habitat complexity metrics as distance from subject changes, between the action camera and DSLR camera systems.

TESTABLE HYPOTHESES

H1: Reprojection error of action camera derived photogrammetry models will be significantly greater than DSLR derived photogrammetry models of the same area.

H2: Spatial error of action camera derived photogrammetry models will be significantly greater than DSLR derived photogrammetry models of the same area.

H3: GSD of action camera derived photogrammetry models will be significantly greater than DSLR derived photogrammetry models of the same area.

H4: Tie point density of action camera derived photogrammetry models will be significantly smaller than DSLR derived photogrammetry models of the same area.

H5: Cloud point density of action camera derived photogrammetry models will be significantly smaller than DSLR derived photogrammetry models of the same area.

H6: Mesh face density of action camera derived photogrammetry models will be significantly smaller than DSLR derived photogrammetry models of the same area.

H7: Point Cloud distances (M3C2) between action camera derived photogrammetry models and DSLR derived photogrammetry models of the same area will be significant.

H8: Slope of action camera derived photogrammetry models and DSLR derived photogrammetry models of the same area be significantly different.

H9: VRM of action camera derived photogrammetry models and DSLR derived photogrammetry models of the same area be significantly different.

H10: Curvature of action camera derived photogrammetry models and DSLR derived photogrammetry models of the same area be significantly different.

H11: Surface complexity of action camera derived photogrammetry models and DSLR derived photogrammetry models of the same area be significantly different.

H12: Distance from the subject will have a greater effect on the quality metrics of the action camera derived photogrammetry models than those generated by the DSLR.

H13: Distance from the subject will have a greater effect on the structural metrics of the action camera derived photogrammetry models than those generated by the DSLR

METHODS

STUDY SITES

Shallow water snorkel surveys were conducted along the nearshore coral reef habitat at Laehala (19°44′15″ N, 155°1′54″ W) in the Hawaiian land division of Honohononui along the Keaukaha coastline in Hilo, Hawai‘i Island (Figure 1). This reef is characterized by patchy coral rubble, turf algae, and interspersed coral communities largely dominated by large *Porites lobata* colonies. This] reef habitat is largely isolated from the ocean during low tide and experiences tidal flush during high tide. Data collection occurred here from 6/15/2022 to 7/15/2022 during mid to high tides when water depth was sufficiently deep to snorkel with a distance of at least 0.5 m between the top of a coral colony and the camera lens (1-2 m water depth). A site selection approach was used to ensure a facsimile of coral reef habitat typically surveyed by divers employing SfM. Selected areas were composed of moderately structural complex benthos, at least one large (~0.5m diameter) coral colony, and a depth that allowed the diver to survey without bringing the camera outside of the water. 15 sites were surveyed using both camera platforms and had an average area of 25m^2. For each of the 15 sites , a snorkeler gathered images following a boustrophedonic (back-and-forth) pattern, ensuring consecutive photographs and video overlap by approximately 70-80%. At least two 0.5m ground control points (GCP) were placed at two opposing corners of a survey plot. Color calibration charts were placed in the survey area to facilitate accurate white balancing.

Deeper surveys were conducted using SCUBA off the Māhukona Hawaiian land division (20°10′49″N 155°54′05″W) along the west Kohala coastline in Waimea, Hawai‘i Island (Figure 1). The nearshore reef in this area extends from the coastline at a very slight slope until roughly 1000ft offshore where it begins to drop off. This area was characterized by rubble-based reefs interspersed with occasional sand grooves. The reef shelf is relatively flat and maintains a shallow depth of roughly 40ft until it begins to drop off. Data collection occurred here on 3/4/2023 and three sites were surveyed at four different distances from the subject (1m, 3m, 6m, 9m). The subject of each survey was centered around a coral structure, similar that of the areas surveyed in Laehala. Image collection was conducted in the same manner as the snorkel surveys wherein the diver deployed GCPs, white balanced off a white dive slate, and collected images in a boustrophedonic pattern with the cameras directed nadir. The diver began 1m from the subject then ascended in the water column to the next distance, using a diver computer to calculate distance from the subject. An additional 9 dive surveys were conducted using scuba on 6/20/2023 and 6/27/2023 off Leleiwi in the Hawaiian land division of Waiakea along the Keaukaha coastline in Hilo, Hawai‘i Island (19° 44' 2.08726" N, 155° 0' 58.19" W) (Figure 1.).

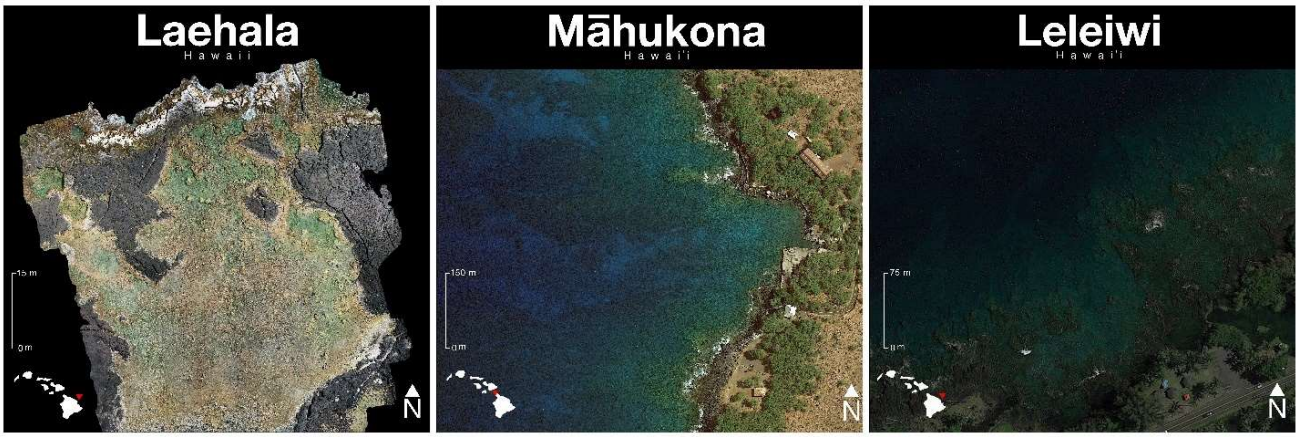

Figure 1. The left map is an aerial view of Laehala, HI, a large North facing tide pool on the East side of the Big Island of Hawaii. The middle map is satellite imagery of the reef area directly nearshore Māhukona, HI (Satellite imagery from Google Earth). The right map is satellite imagery of the nearshore dive location Leleiwi, HI (Satellite imagery from Google Earth).

CAMERA PLATFORMS

Divers collected images on a DSLR and action camera simultaneously. Both DSLR images were collected by a diver operating a Canon EOS 60D with a Canon EF-S 18-55mm f/3.55-5.6 IS SLR lens within a polycarbonate Ikelite housing fitted with a 6-inch dome port. DSLR settings were set to manual shooting mode (f/11, 1/320, 400 ISO, and zoom set to 24mm). Action camera video was collected using a GoPro Hero4 with an unmodified 2.92mm prime lens within a polycarbonate, flat lensed housing. The action camera was set to video mode with resolution set to 4k (2160p), capture rate 60 frames per second, and white balance set to Auto to compensate for variable conditions. In video mode, the GoPro Hero4 uses automatic exposure balancing (f/2.8, auto shutter, auto ISO). The action camera was mounted on the top of the DSLR housing as pictured in Figure 2, allowing for both image and video to be collected simultaneously from the same perspective. Only ambient light was used for illumination. For the snorkel surveys at Laehala, divers collected imagery of a single area once. For the SCUBA based dives at Mahukona and Leleiwi, the same area was surveyed 4 times, each at a different distance from the subject (1m, 3m, 6m, 9m). Accurately collecting imagery at a set distance from a nadir subject necessitated dives on SCUBA.

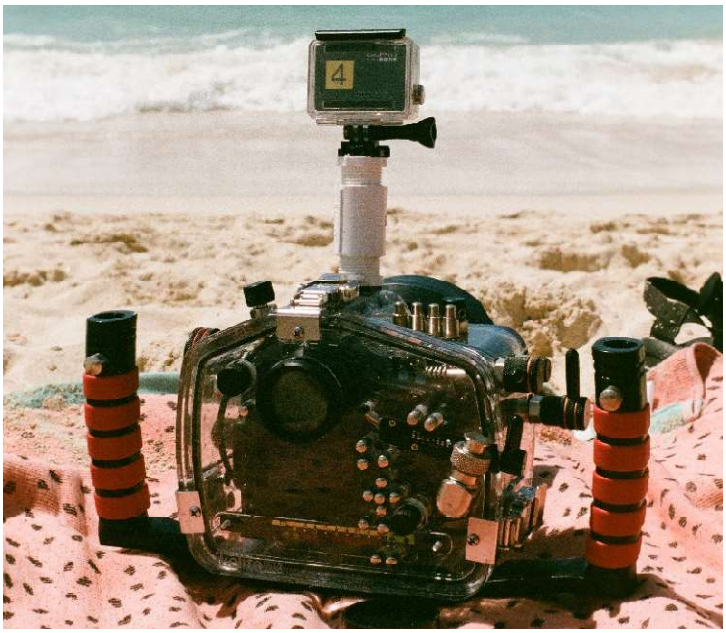

Figure 2. Dual camera rig for simultaneous capture of action camera (GoPro Hero4) video and DSLR (Canon EOS 60D) photo capture. The homemade PVC riser mount for the action camera on the top of the housing prevents the dome of the housing to be included in the wide frame of the GoPro Hero4 while allowing simultaneous image collection of the same area.

DATA PROCESSING

Models were rendered in Agisoft Metashape v.1.7.1 (Agisoft LLC, St. Petersburg. Russia) following techniques created specifically for 3D reconstructions from coral reef habitats as described in Burns et al. (2015). Raw video footage from the GoPro Hero4 was converted into still images using FFmpeg v.4.4 (FFmpeg 2022). With consideration to DSLR in-situ image collection, still images were extracted at 2 frames per second to ensure a 70-80% overlap for sequential action camera images. This also allowed for the removal of potentially error inducing images where the diver is repositioning themselves. Approximately 100-200 images were captured on each camera platform for a $30m^2$ area. GoPro Hero4 images collected in deeper water across the depth spectrum (1m, 3m, 6m, 9m) required color correction beyond the automatic setting. Images for deep GoPro Hero4 plots were white balanced off the slate in Adobe Photoshop Lightroom v.6 (Adobe 2023). Images were loaded into Agisoft Metashape and aligned into a tie point cloud (adaptive fitting=true, keypoint limit=50000, mask tiepoints=false, tiepoint limit=5000). The sparse tie point cloud was refined further using stereo overlap and texture to produce a dense point cloud. Adjacent dense points were connected to nearest neighbors creating a polygon mesh. Raw imagery was overlaid on the mesh, producing an accurate 3D (texture size=16384). A rectangular polygon was drawn around the scale bars in each 3D model and used to crop the digital elevation model (DEM) for export. Cropped DEMs were exported at 1cm/pixel and 1mm/pixel

resolutions for each of the 120 total 3D models. To prep data for the point cloud comparison, dense point clouds were exported from Agisoft Metashape into CloudCompare v2.13.alpha (CloudCompare 2022). Paired point clouds were roughly aligned using the scale bars in the corresponding plots and then refined using the fine registration tool.

ANALYSES

Statistical analyses were completed in the statistical software R v.4.3.0 (R core team 2023) running in RStudio v.2023.03. Spatial error and reprojection error and GSD values were derived from Agisoft model reports. Densities for tie points, point clouds, and mesh faces were calculated using the area for each corresponding plot. Point cloud distances for paired plots were calculated in CloudCompare using the Multiscale Model-to-Model Cloud Comparison (M3C2) plugin following methods established in Lague, Brodu, & Leroux (2013). M3C2 is an algorithm that works by comparing the normal vectors of corresponding points in two point cloud models. It quantifies the differences between the models and generates a color map that represents these discrepancies. Distance data was exported from CloudCompare. Individual distances are reported as positive or negative to indicate the discrepancy in relation to the reference cloud. To calculate an accurate mean and median, the absolute value of all distances was computed. Metrics of 3D habitat complexity were calculated in R on DEMs for corresponding plots using methods established in Fukunaga et al. (2019). This approach produced values of slope, VRM, curvature, and surface complexity. For overall 3D model quality metrics and 3D habitat structure metrics, a paired Students t test was performed for each survey between the two camera platforms. A one tailed t test was performed for the 3D model quality metrics with the alternative hypothesis assuming superior quality from DSLR produced models. For 3D habitat structure metrics, a two tailed t test was performed between each pair of 3D models. To investigate the effect of distance on the data parameters, the data was subset into two categories; close to the subject (1-3m) and far from the subject (6-9m). A sign test was performed on the paired metrics at the close and far distances to compare data between these depth categories.

RESULTS

IMAGES AND MODELS

Models generated from the 1-3m distance-from-substrate exhibited a a moderate difference in image quality between the two platforms. The images from the GoPro suffered from chromatic aberration and distortion towards the edge of the images when compared to images collected on the Canon 60D (Figure 3). The lower resolution of the GoPro images resulted in over exposed images with poor sharpness compared to those collected using the 60D (Figure 3). Additionally, models built on near subject images produced by the GoPro Hero4 tended to encapsulate a larger spatial area since the fisheye lens has a wider field of view, however the lens distortion detrimentally affected sharpness and contrast in comparison to the 60D derived models (Figure 4). This difference, particularly the sharpness, significantly worsened with increasing distance from the subject in comparison to the 60D (Figure 4).

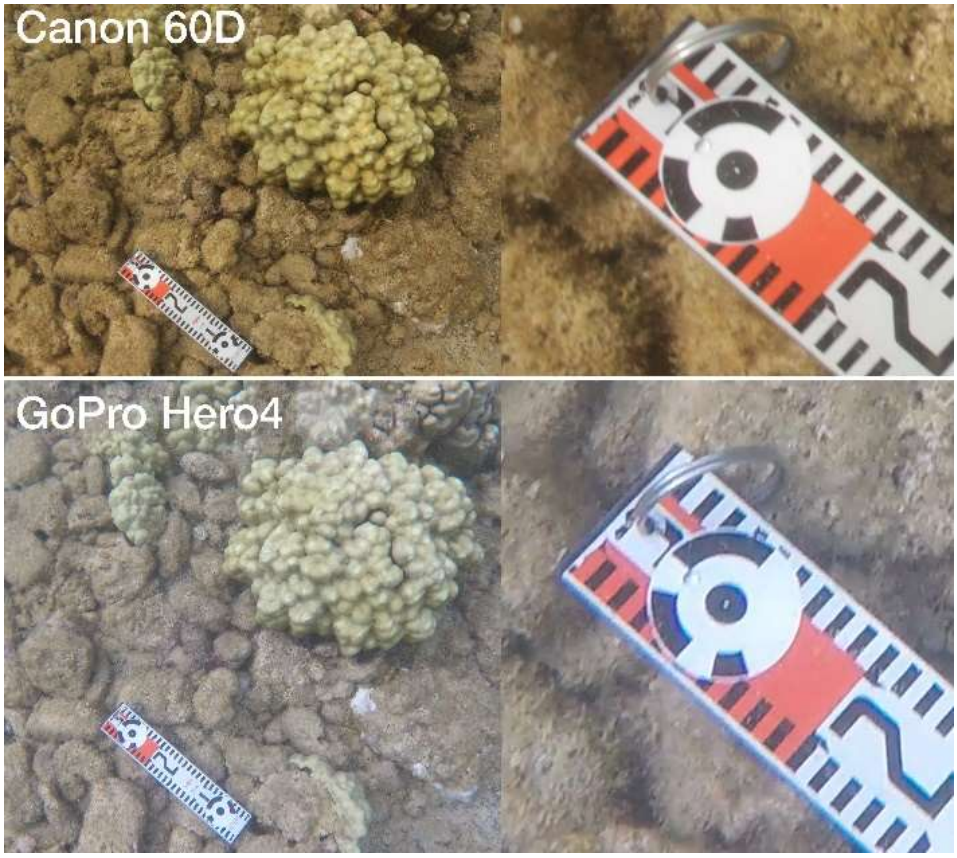

Figure 3. Comparison of images collected at the same location and time between the two camera platforms (Canon 60D and GoPro Hero4).

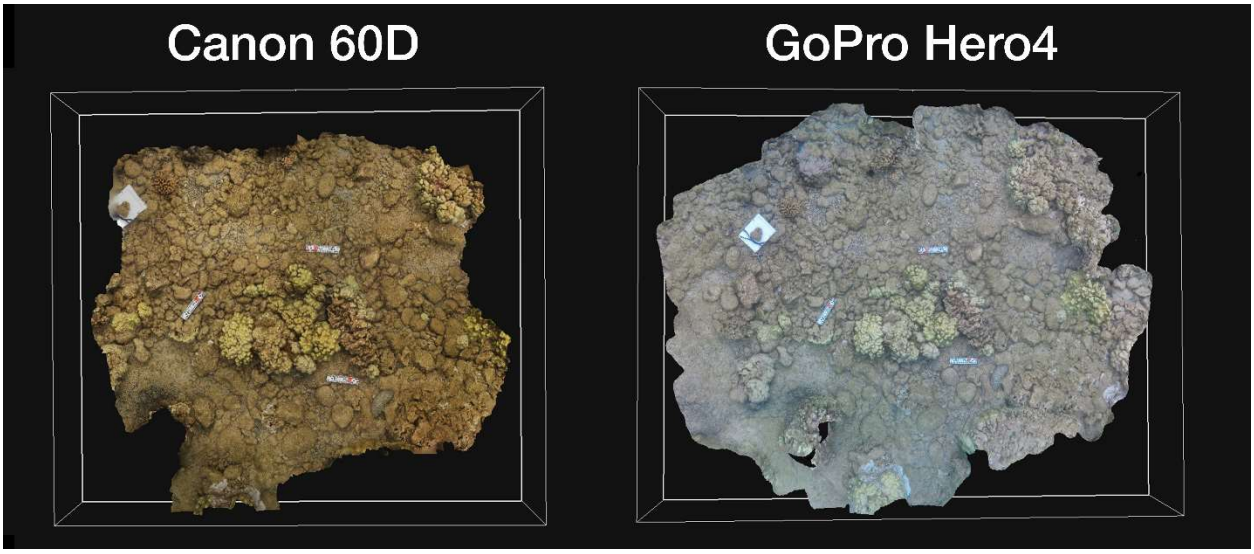

Figure 4. Comparison of 3D models generated from images collected between two camera platforms (Canon 60D and GoPro Hero4).

3D MODEL QUALITY METRICS

Overall, the 3D models quality metrics from paired models were significantly worse for the GoPro Hero4 in comparison to the Canon 60D. Both spatial error and reprojection error were significantly lower for paired models generated by the Canon 60D than the GoPro Hero4 (Spatial error: DF = 61, t= -2.72, p = 0.00429. Reprojection error: DF = 61, t= -9.98, p = 9.68e-15. Figure 5.). GSD was also significantly lower for paired models generated by the Canon 60D when compared the those generated by the GoPro Hero4 (GSD: DF = 61, t= -10.58, p = 0. 9.89e-16. Figure 6). Tie point, point cloud, and mesh face densities were significantly larger for models generated by the Canon 60D for paired models (Tie point density: DF = 61, t= 2.66, p = 0.00495. Point cloud density: DF = 61, t= 6.19, p = 2.82e-08, Mesh face density: DF = 61, t= 5.95, p = 7.07e-08. Figure 7). Across 21 paired models and nearly 310 million point cloud measurements, the median distance was 0.60547cm and the mean difference was 0.88065cm (Figure 8).

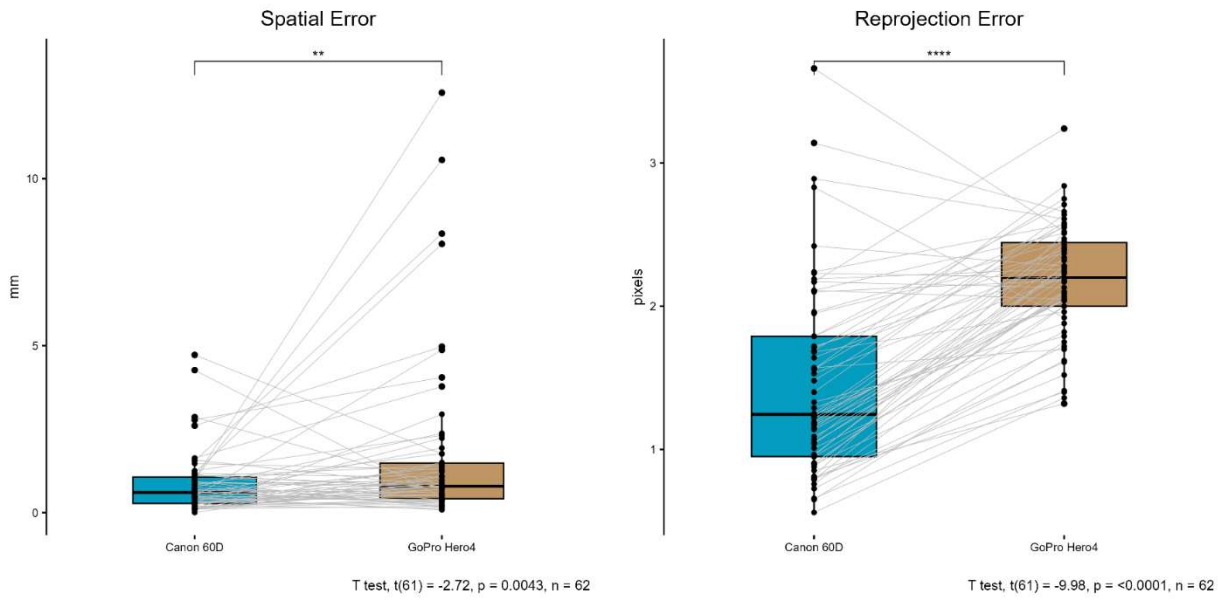

Figure 5. Comparison of spatial error in mm and reprojection error in pixels between paired models collected by a Canon 60D and GoPro Hero4.

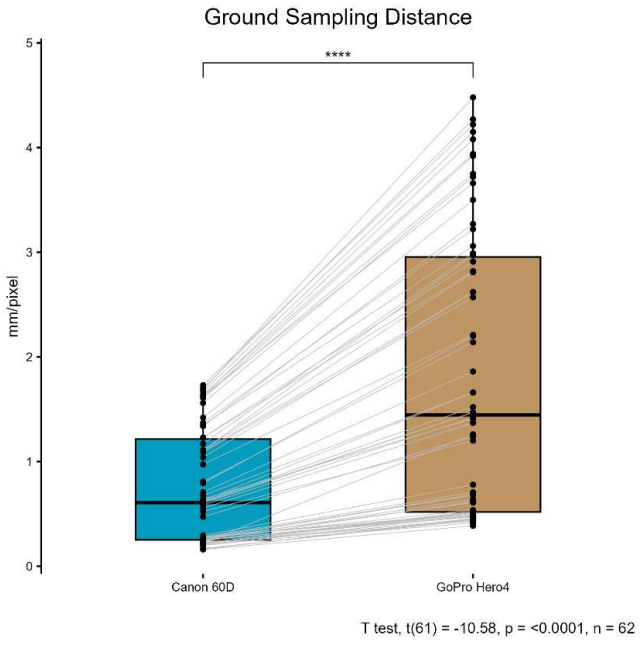

Figure 6. Comparison of ground sampling distance (GSD) values in mm/pixel between paired models collected by a Canon 60D and GoPro Hero4.

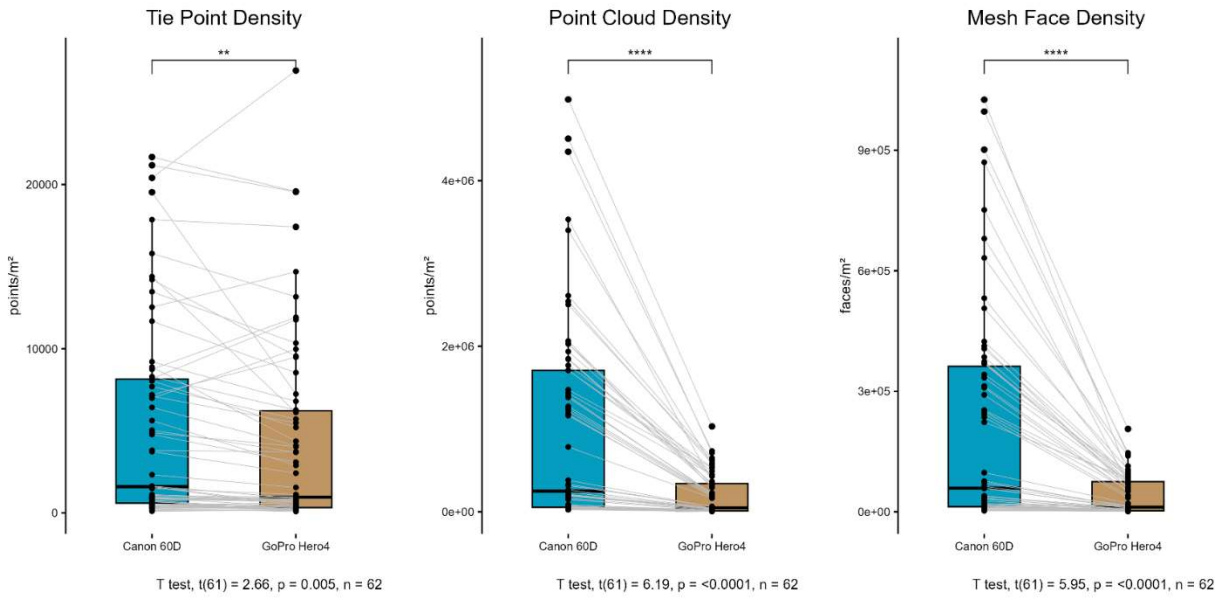

Figure 7. Comparison 3D model attributed densities between paired surveys using Canon 60D and GoPro Hero4.

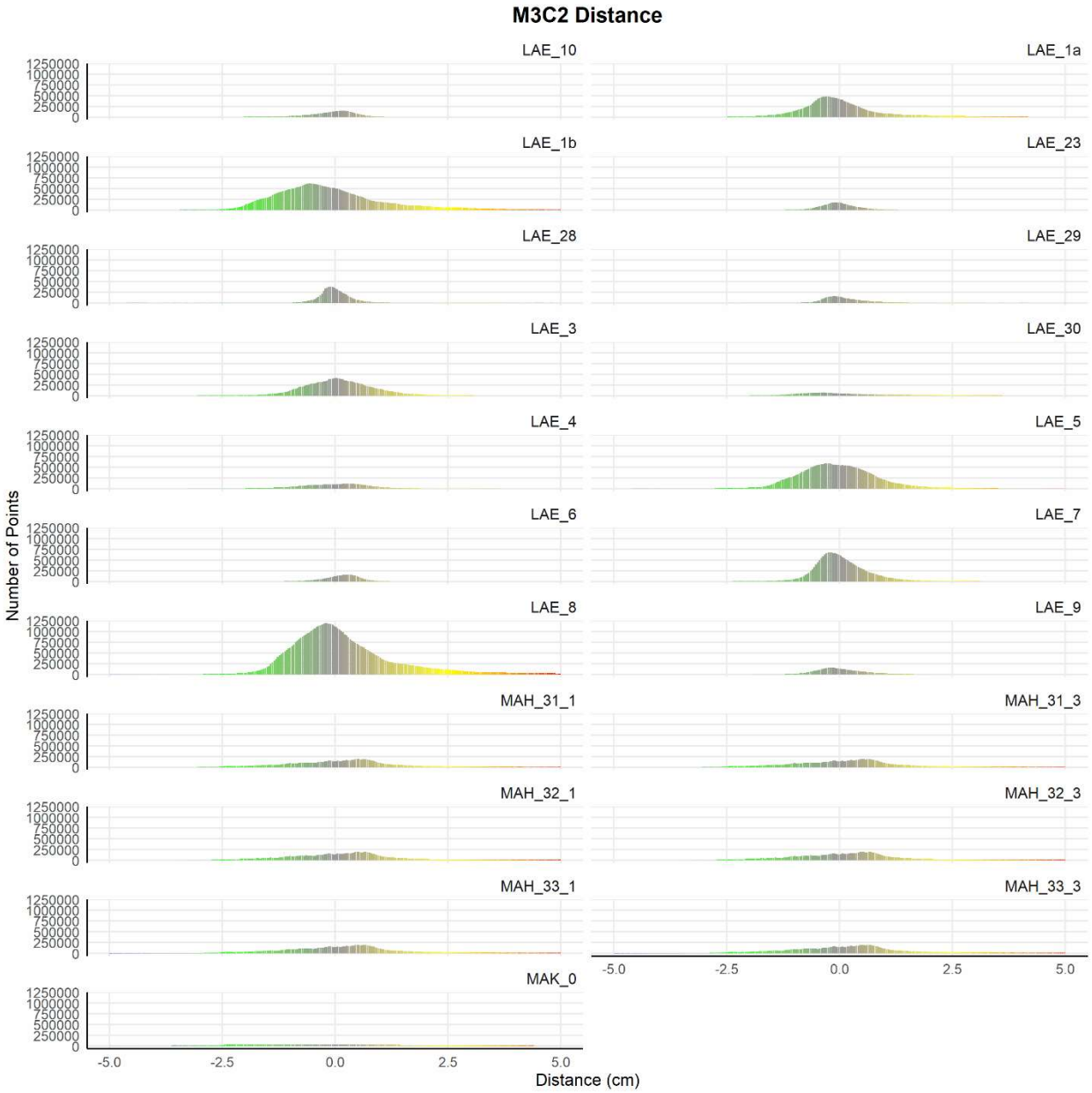

Figure 8. Comparison of M3C2 distances in cm from paired models collected for the same survey at collected at close distance (1-3m) between two camera platforms (Canon 60D and GoPro Hero4).

3D HABITAT STRUCTURE METRICS

All 3D habitat metrics, except curvature, were significantly different between platforms for paired DEMs at both 1cm/pixel (Slope: DF = 61, t= 6.18, p = 5.71e-08. VRM: DF = 61, t= 13.56, p = 4.60e-20. Curvature: DF = 61, t= -0.38, p = 0.707. Surface Complexity: DF = 61, t= 9.96, p = 2.05e-14. Figure 9.) and 1mm/pixel cell resolutions (Slope: DF = 61, t= 6.06, p = 9.09d-08. VRM: DF = 61, t= 7.63, p = 1.91e-10. Curvature: DF = 61, t= -1.02, p = 0.311. Surface Complexity: DF = 61, t= 8.3, p = 1.33e-11. Figure 10.). For DEMs at 1cm/pixel, the Canon 60D had greater median values for slope, VRM, and surface complexity. For curvature, the Canon 60D had a median value slightly closer to 0 than the GoPro Hero4. For DEMs exported at 1mm/pixel, these relationships remained consistent but more outliers were generated for the Canon 60D in terms of curvature.

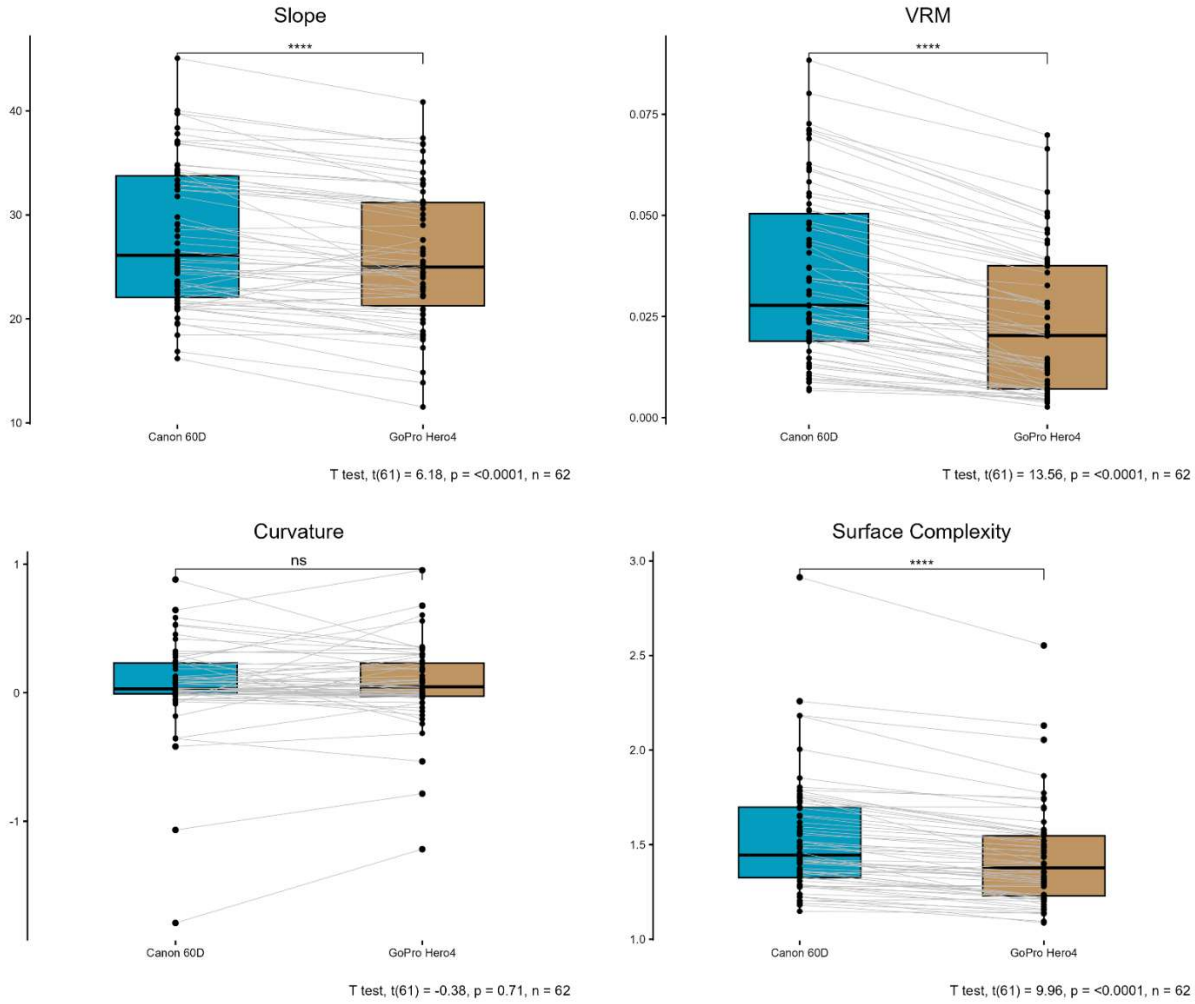

Figure 9. Comparison 3D structure metrics calculated using a 1cm/pixel DEM between paired surveys using Canon 60D and GoPro Hero4.

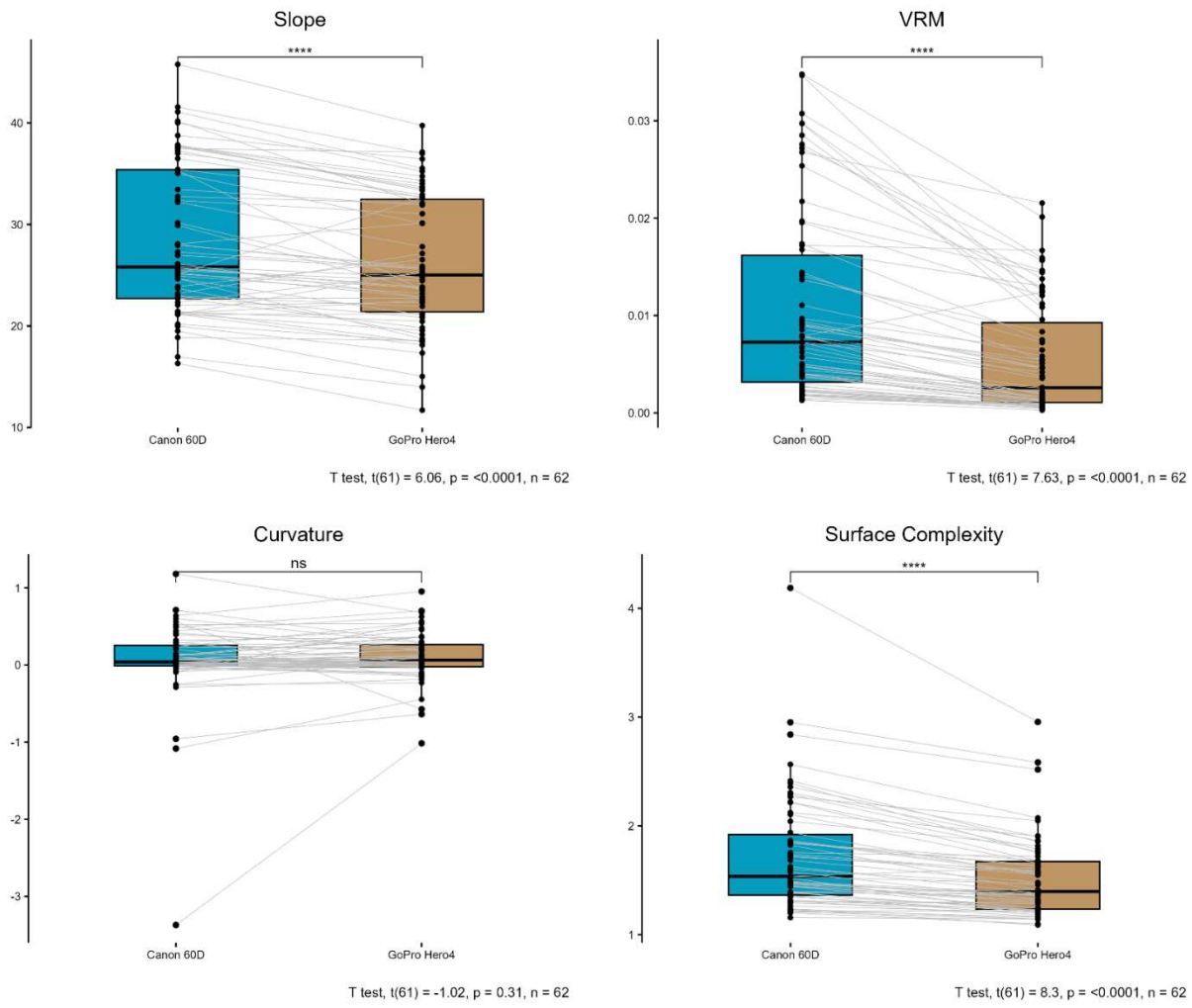

Figure 10. Comparison 3D structure metrics calculated using a 1mm/pixel DEM between paired surveys using Canon 60D and GoPro Hero4.

DISTANCE FROM SUBJECT

3D model quality metrics from paired surveys between two camera platforms (Canon 60D and GoPro Hero4) at two distance categories (1-3m and 6-9m) exhibited more complex discerning differences between the two camera systems. . Spatial error was not significantly different between platforms at close a distance but was significantly greater for the GoPro at far distances (Spatial error (1-3m): DF = 23, S = 0.375, p = 0.154. Spatial error (6-9m): DF = 22, S = 0.261, p = 0.0173. Figure 11.). Reprojection error was significantly greater in paired models generated by the GoPro Hero4 for both distance categories (Reprojection error (1-3m): DF = 23, S = 0.0417, p = 1.49e-06. Reprojection error (6-9m): DF = 22, S = 0.304, p = 0.0466. Figure 12.). GSD was significantly greater in paired models generated by the GoPro Hero4 for both distance categories (GSD (1-3m): DF = 23, S = 0, p = 5.96e-08. GSD (6-9m): DF = 22, S = 0 , p = 1.19e-07. Figure 13.). Tie point density was significantly smaller in paired models generated by

the GoPro Hero4 for both distance categories (Tie point density (1-3m): DF = 23, S = 0. 0.917, p = 1.79e-05. Tie point density (6-9m): DF = 22, S = 0.826, p = 0.0013. Figure 14.). Point cloud density was significantly smaller in paired models generated by the GoPro Hero4 for both distance categories (Point cloud density (1-3m): DF = 23, S = 1, p = 5.96e-08. Point cloud density (6-9m): DF = 22, S = 1, p = 1.19e-07. Figure 15.). Mesh face density was significantly smaller in paired models generated by the GoPro Hero4 for both distance categories (Mesh face density (1-3m): DF = 23, S = 1, p = 5.96e-08. Mesh face density (6-9m): DF = 22, S = 1, p = 1.19e-07. Figure 16).

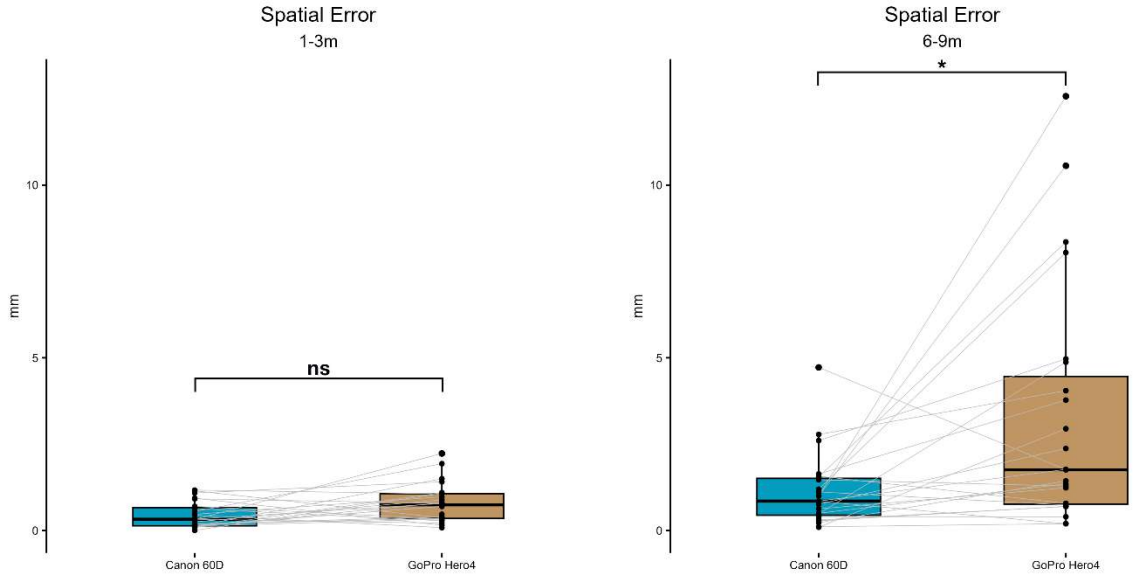

Figure 11. Comparison of spatial error at 1-3m from subject and 6-9m from subject for paired surveys using Canon 60D and GoPro Hero4.

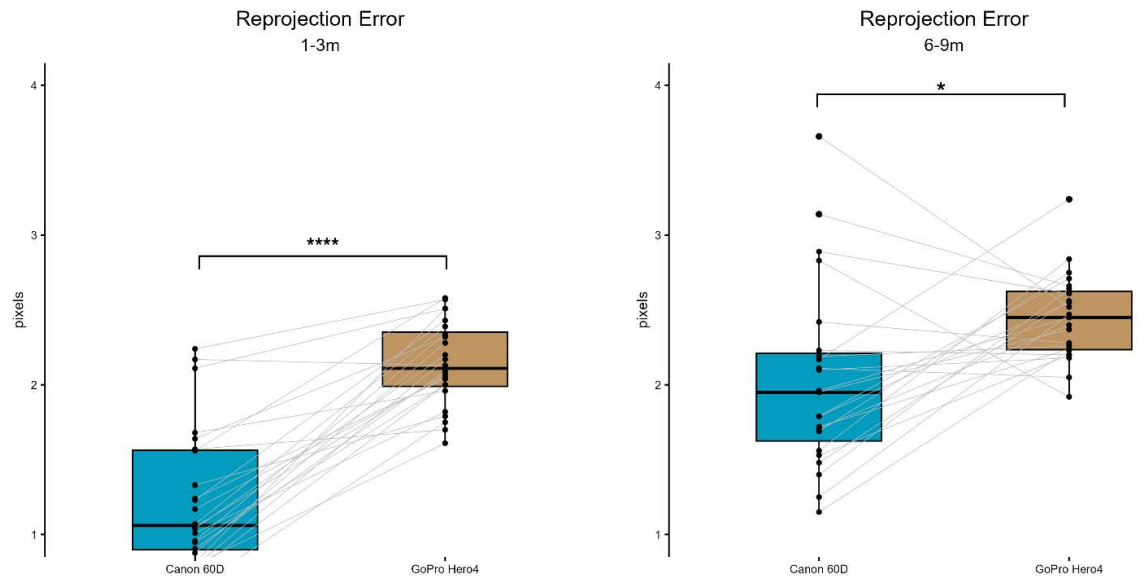

Figure 12. Comparison of reprojection error at 1-3m from subject and 6-9m from subject for paired surveys using Canon 60D and GoPro Hero4.

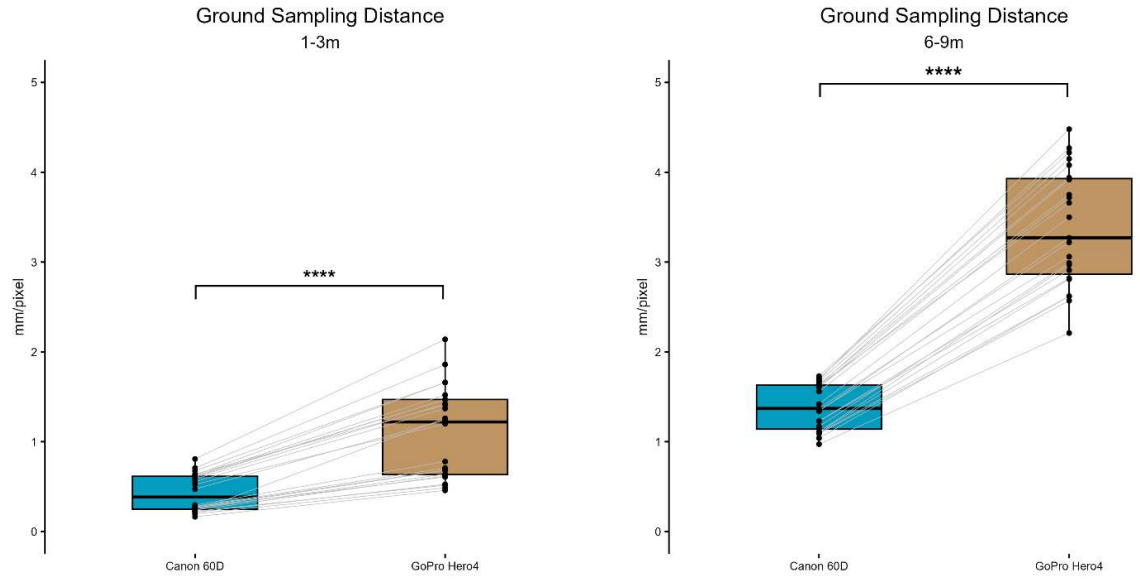

Figure 13. Comparison of GSD at 1-3m from subject and 6-9m from subject for paired surveys using Canon 60D and GoPro Hero4.

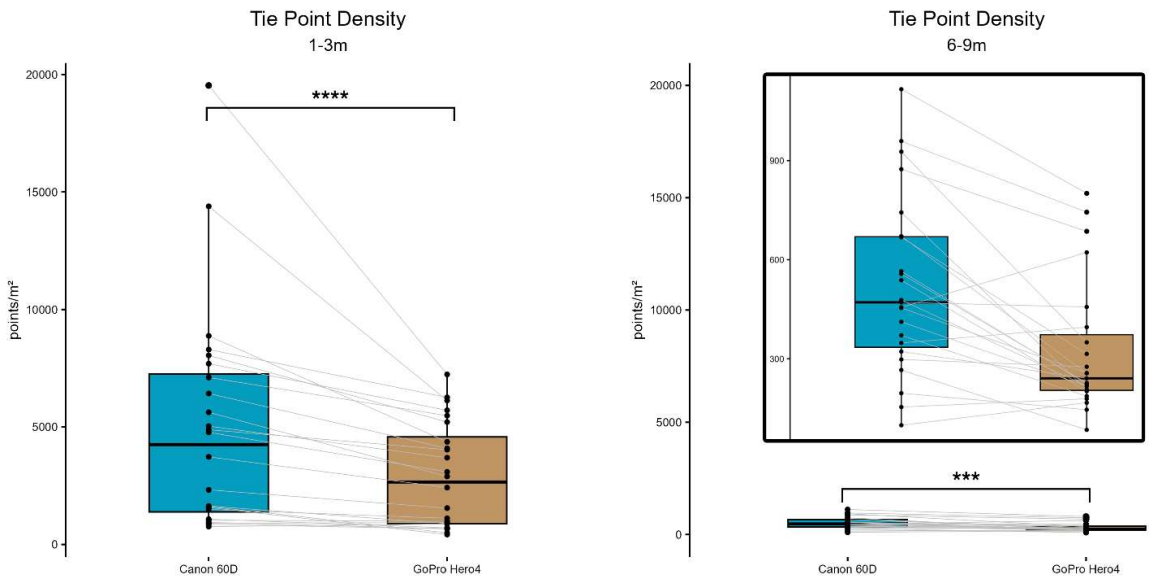

Figure 14. Comparison of tie point density at 1-3m from subject and 6-9m from subject for paired surveys using Canon 60D and GoPro Hero4.

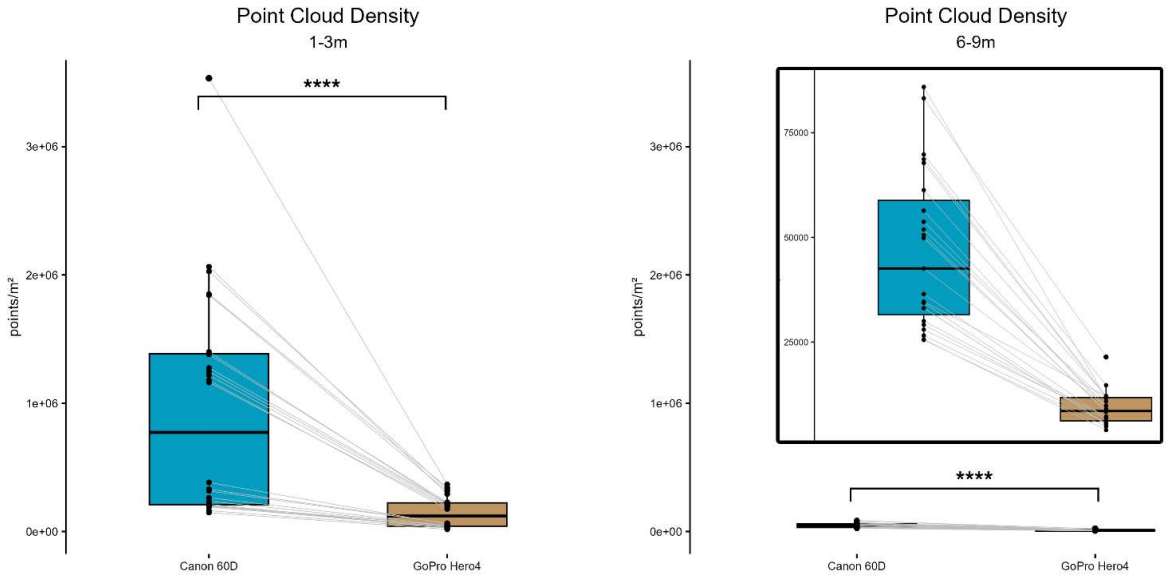

Figure 15. Comparison of point cloud density at 1-3m from subject and 6-9m from subject for paired surveys using Canon 60D and GoPro Hero4.

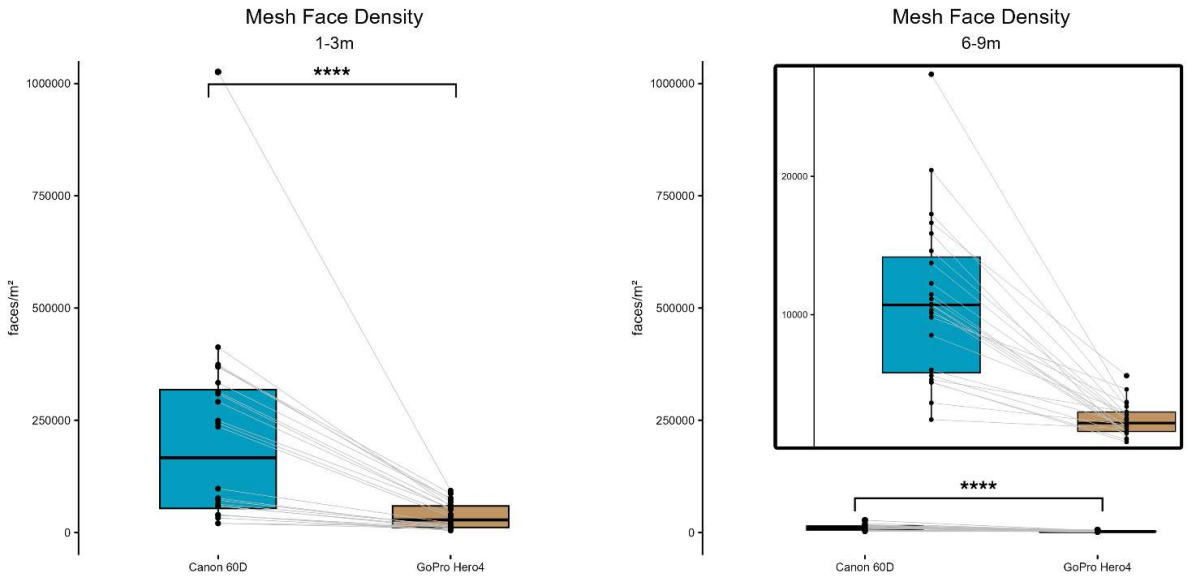

Figure 16. Comparison of mesh face density at 1-3m from subject and 6-9m from subject for paired surveys using Canon 60D and GoPro Hero4.

3D habitat structure metrics from paired surveys between two camera platforms (Canon 60D and GoPro Hero4) at two distance categories (1-3m and 6-9m) exhibited a more complex relationship as well. Additionally, this comparison was done on a DEM exported at 1cm/pixel and one at 1mm/pixel. For both DEM scales, slope was significantly different at 1-3m but not significantly from 6-9m between the two camera platforms (Slope 1cm (1-3m): DF = 23, S = 0.917, p = 3.59e-05. Slope 1cm (6-9m): DF = 22, S = 0.609, p = 0.405. Slope 1mm (1-3m): DF = 23, S = 0.917, p = 3.59e-05. Slope 1mm (6-9m): DF = 22, S = 0.696, p = 0.0931. Figure 17.). VRM was significantly different between the two camera platforms at different DEM scales and distance categories (VRM 1cm (1-3m): DF = 23, S = 1, p = 1.19e-07. VRM 1cm (6-9m): DF = 22, S = 1, p = 2.38e-07. VRM 1mm (1-3m): DF = 23, S = 1, p = 1.19e-07. VRM 1mm (6-9m): DF = 22, S = 1, p = 2.38e-07. Figure 18.). Curvature was not significantly different between paired models generated by the Canon 60D or GoPro Hero4 for either distance categories or DEM scales (Curvature 1cm (1-3m): DF = 23, S = 0.542, p = 0.839. Curvature 1cm (6-9m): DF = 22, S = 0.652, p = 0.21. Curvature 1mm (1-3m): DF = 23, S = 0.333, p = 0.152. Curvature 1mm (6-9m): DF = 22, S = 0.652, p = 0.21. Figure 19.). Surface complexity was significantly different in paired models between two camera platforms for both distance categories and DEM scales (Surface complexity 1cm (1-3m): DF = 23, S = 0.958, p = 2.98e-06. Surface complexity 1cm (6-9m): DF = 22, S = 0.913, p = 6.60e-05. Surface complexity 1mm (1-3m): DF = 23, S = 0.958, p = 2.98e-06. Surface complexity 1mm (6-9m): DF = 22, S = 0.957, p = 5.72e-06. Figure 20.).

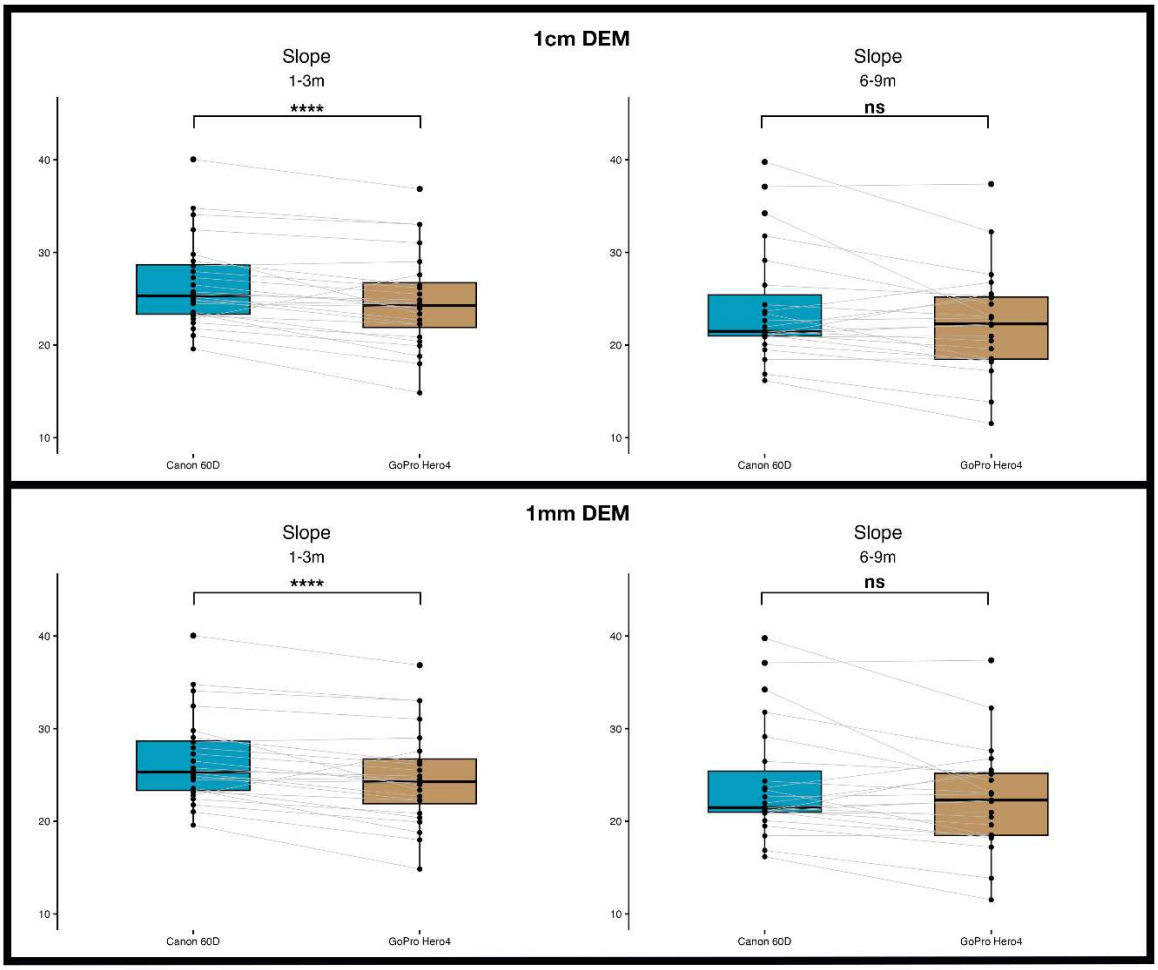

Figure 17. Comparison of slope between paired models generated by a Canon 60D and GoPro Hero4 at 1-3m from subject and 6-9m from subject for a DEM export at 1cm/pixel and 1mm/pixel.

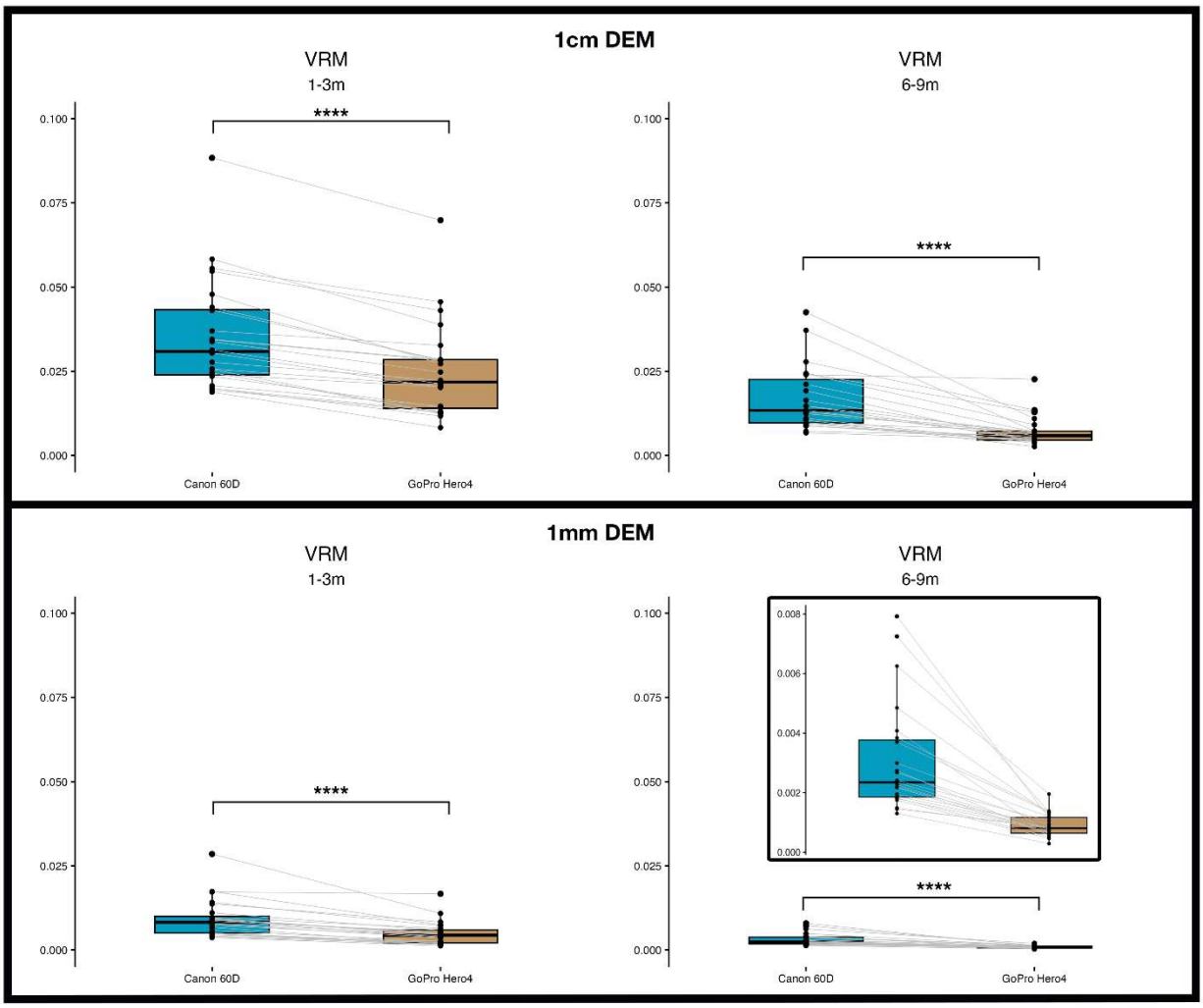

Figure 18. Comparison of VRM between paired models generated by a Canon 60D and GoPro Hero4 at 1-3m from subject and 6-9m from subject for a DEM export at 1cm/pixel and 1mm/pixel.

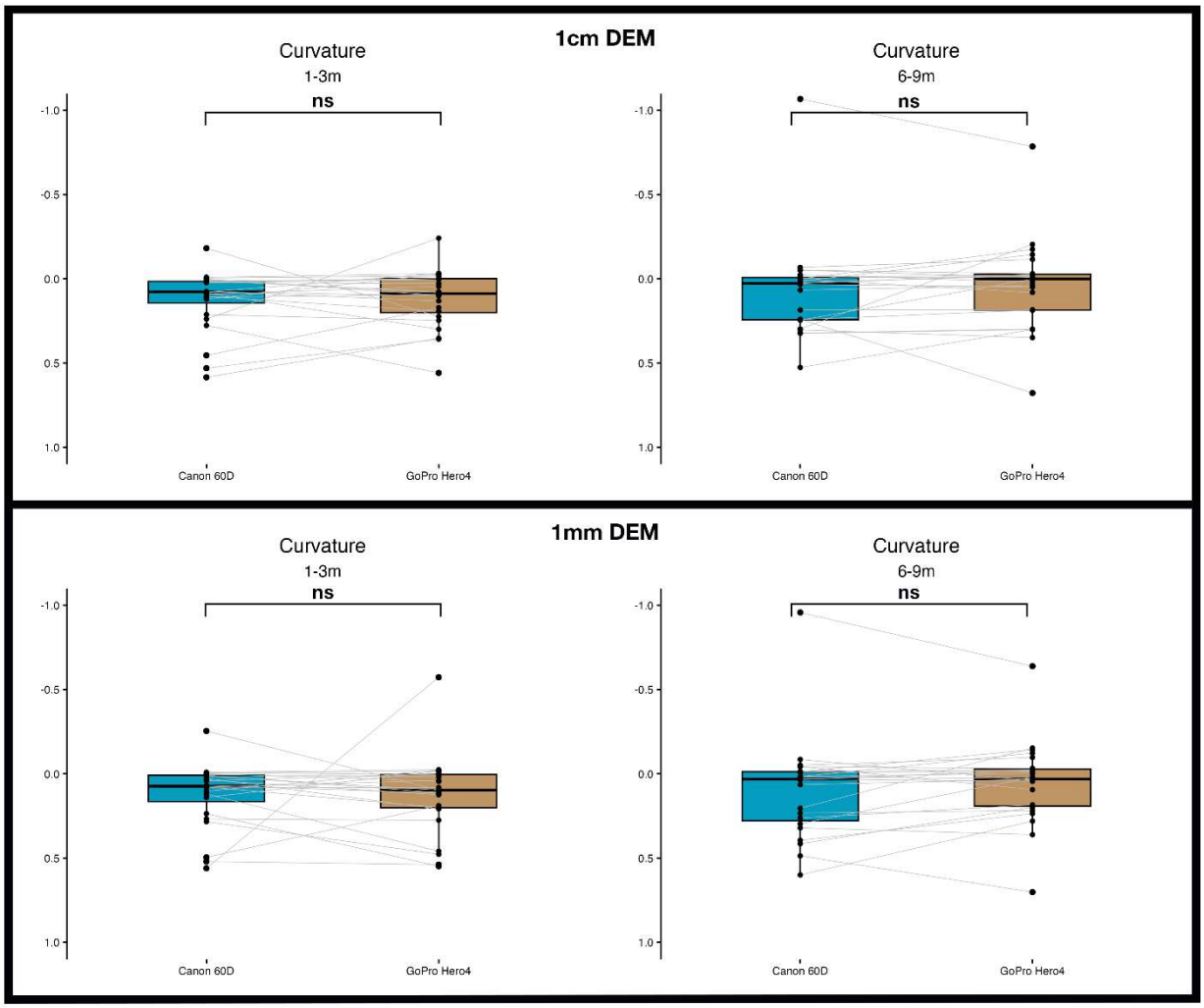

Figure 19. Comparison of curvature between paired models generated by a Canon 60D and GoPro Hero4 at 1-3m from subject and 6-9m from subject for a DEM export at 1cm/pixel and 1mm/pixel.

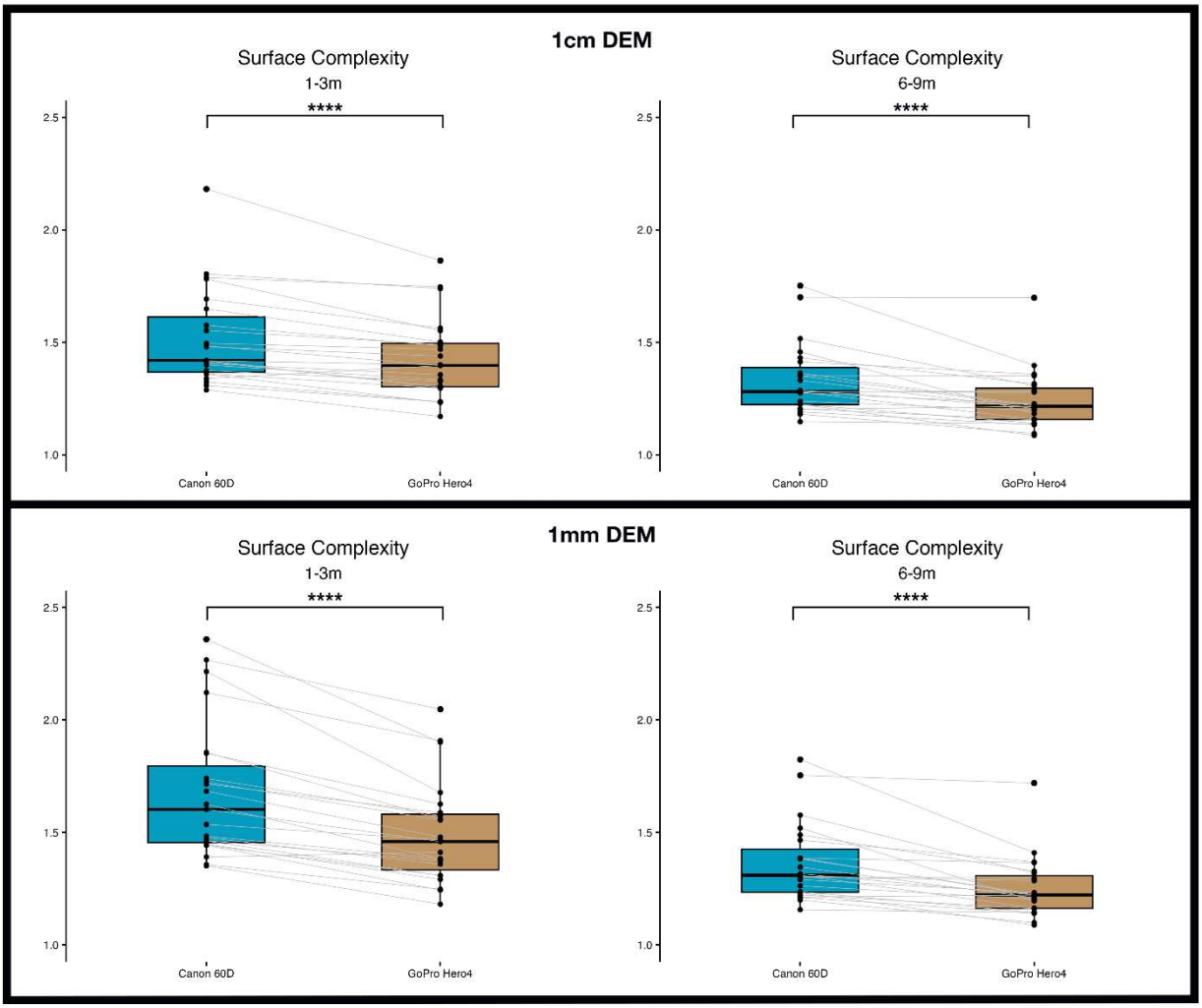

Figure 20. Comparison of surface complexity between paired models generated by a Canon 60D and GoPro Hero4 at 1-3m from subject and 6-9m from subject for a DEM export at 1cm/pixel and 1mm/pixel.

DISCUSSION

IMAGES AND MODELS

Images from the Canon 60D had more visual richness and clarity (Figure 4). This is an inevitable result based on the sensor size difference between the two platforms. The Canon 60D sensor is nearly 250% larger than the sensor in the GoPro Hero4 (26.8mm vs 7.66mm) and a sensor with greater surface area means a greater number of photos are captured. This smaller sensor limits the dynamic range, leading to images that appear brighter and less contrasted. A larger sensor with more pixels can capture more photons, resulting in a higher signal-to-noise ratio (SNR). This means that the image signal will be stronger compared to the inherent noise, resulting in a cleaner and better-exposed image. The noise, which includes electronic noise, thermal noise, and shot noise, remains relatively constant regardless of sensor size. Due to the higher signal level, the noise becomes a smaller percentage of the overall signal, leading to a higher SNR and lower noise levels in the final image (Carlson 2002).

Images from the Hero4 were troubled with severe chromatic aberration and distortion towards the edge of the frame. This is particularly noticeable in the scale bar closeup in Figure 4. Chromatic aberration can certainly be induced by the small image sensor and onboard processing onboard the Hero4 but it's also hindered by a very short focal length (2.92 mm) and a fixed aperture of f/2.8. Short wide angle lenses like the fisheye lens on the Hero4 are particularly prone to lateral chromatic aberration because light rays from the edges of the frame strike the lens at steeper angles compared to light rays from the center (Menna et al. 2018). This increased angle of incidence at the lens periphery can exacerbate the dispersion of different colors, causing chromatic aberration to become more noticeable towards the edges of the image. Different colors of light have different wavelengths and refract differently when passing through a lens. The amount of refraction varies based on the wavelength of the light. As a result, different colors do not converge at the same focal point and "ghost" in the produced image. The fixed f/2.8 aperture on the Hero4 means that exposure control is dictated by the shutter speed and ISO, both of which are adjusted automatically in video mode. This dynamic adjustment seemed to frequently overexpose the images indicating that the Hero4 exposure control algorithms might prioritize avoiding underexposure.

Motion blur wasn't a significant issue for either platform but some motion blur was present in some images for many of the plots. Typically divers using DSLRs to collect SfM imagery rely on manually releasing the shutter and timing the frequency of release with their travel speed. This allows them to ensure there's enough coverage between sequential images without overloading card write speeds or storage. The balance between the speed in which the camera is moving in relation to the subject and the exposure settings determine if any motion blur is produced. If camera moves significantly while the sensor is exposed for a prolonged duration, the image produced will be a collection of all the movement.

The settings used for the Canon 60D are more customizable and would allow for a user to compensate for low light settings or high current environments. The GoPro Hero4 lacks the same exposure customization in video mode. A large amount of images were extracted from FFmpeg even at 2 frames per second. This allowed me to remove images where the camera rig was moving quickly in relation to the subject. More recent GoPro Hero models have a timed shutter release mode which allows for rapid capture of images at a set interval. SfM imagery collected on more recent models following this method might serve as a closer analog to the sequential shutter release of a surveyor using a DSLR. However, the GoPro Hero4 used in this study serves as bottom end baseline in terms of accessibility and implementation.

A precursor to image collection on any SfM photogrammetry project, especially underwater, is white balancing. Most consumer DSLRs allow the user define a custom white balance setting using a reference image. Often times white or grey reference cards are placed in the survey environment, photographed, and used as a corrective reference. One of the largest shortcomings of the GoPro Hero4 is the inability to manually set a custom white balance beyond the preset options. The Hero4 also lacks a screen to reference the appearance of the preset options (Auto, 3000k, 5500k, 6500k) and due to this uncertainty I used the Auto setting to compensate for variable cloud cover, turbidity, and depth. In ambient, sunny, shallow underwater conditions the appearance of the Hero4 was close to the Canon 60D in terms of white balance however the images overall appeared cooler than correctly white balanced sister images on the Canon 60D. For underwater depths around 9m, the automatic white balancing on the Hero4 is unable to correct for the loss of light and the video appears quite blue. Image frames were extracted using FFmpeg and manually corrected in Adobe Photoshop Lightroom. The majority of the color was recovered but since the images are compressed JPEGs, detail was lost. Model building was attempted on both corrected and uncorrected images but performance and model quality was greatly improved with the color corrected images.

3D MODEL QUALITY METRICS

For all 62 paired 3D models, 3D model quality metrics were significantly worse for the GoPro Hero4 compared to the Canon 60D. With respect to reprojection error, the GoPro had nearly twice the median pixel error when compared to the Canon 60D (Figure 5). Errors in respect to reprojection error might be introduced lens distortion (O'Connor J. 2018). If lens distortion is not properly accounted for during the calibration or reconstruction process, it can introduce errors in the projection of image points onto the 3D model, leading to reprojection errors. Since the GoPro images were produced from frames of 4k video, the metadata which Agisoft Metashape uses to correct for distortion was lost. Without this correction there was a 96% image alignment rate over 10,000 GoPro Hero4 images used to build the respective 3D models.

GSD was much lower or finer for the Canon 60D in comparison to the GoPro Hero4 (Figure 6). GSD is a standard for quality evaluation for photogrammetry derived orthomosaics. GSD is determined by

the distance of the camera or sensor from the subject, the focal length of the camera lens, the size of the produced image, and the pixel size of the image sensor. As the distance from the subject increases or the focal length decreases, the GSD becomes larger, meaning each pixel covers a larger area on the ground. Conversely, as the distance decreases or the focal length increases, the GSD becomes smaller, resulting in higher spatial resolution. The GoPro Hero4 has 66% smaller images, a 92% smaller image sensor, and an 87% shorter focal length. This explains the GSD difference between the two platforms. The 3D reconstruction process estimates the distance between the original images and the resultant point cloud. Using this we can roughly illustrate the linear relationship between GSD and distance from the subject. (Figure 21).

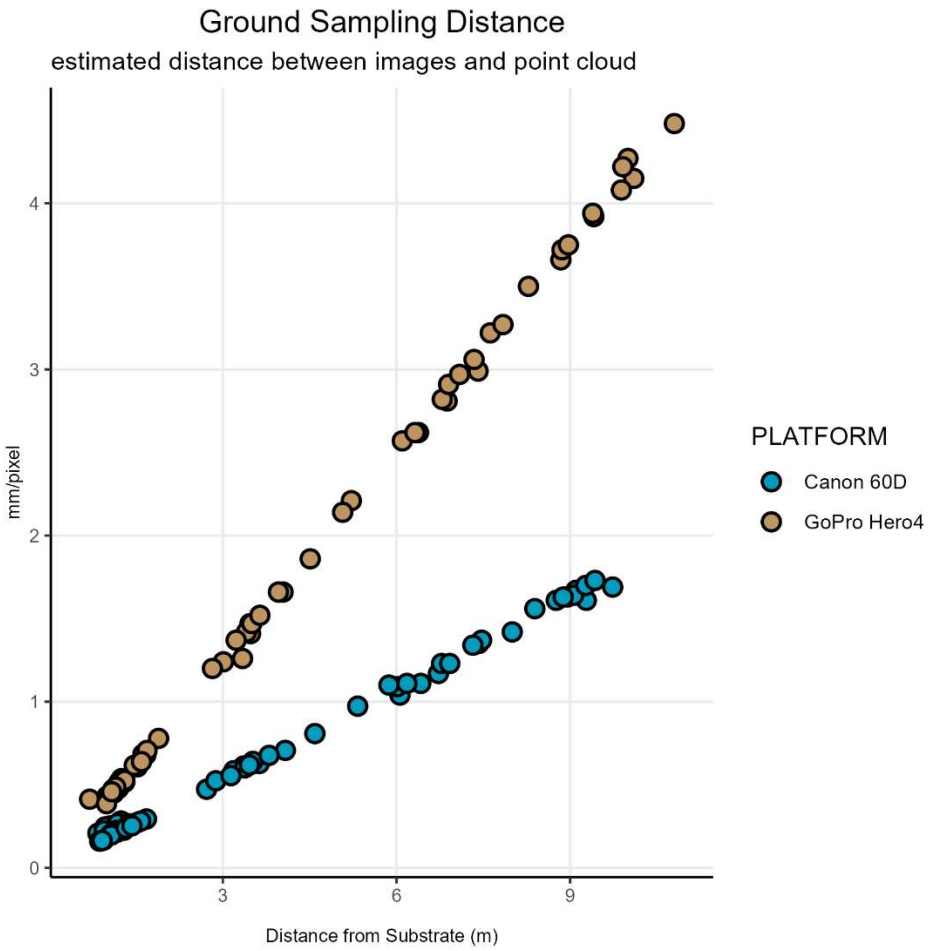

Figure 21. Relationship between ground sampling distance (GSD) and estimated distance between images and reconstructed point cloud for two camera platforms (Canon 60D and GoPro Hero4) n=62.

This illustrates the runaway relationship both cameras have with distance to their subject. If you wanted to get GSD of 1mm/pixel you would need to the be closer than 3m to your subject using the GoPro Hero4. With the Canon 60D you could be as far away as 6m. On the other hand if your limited to only getting access to your subject from 9m away you might expect a GSD of 3.8mm/pixel for a GoPro Hero4, while a Canon 60D might produce an orthomosaic with a GSD of 1.6mm/pixel. This relationship is important to keep in mind with respect to your access and means to a study location.

Tie point density, point cloud density and mesh face densities were all significantly different between the two camera platforms. All of these fundamental parts of a 3D model depend on the image resolution, image overlap, and reconstruction settings. Since the same reconstruction settings were used in Agisoft Metashape for model generation, the only variables are image resolution and overlap. Higher resolution images generally result more tie point matches, and a denser point cloud since they contain more detailed information. The GoPro Hero4 produces images that are 66% smaller than the Canon 60D and this likely accounts for a majority of the difference in the two densities between the platforms. Additionally, increasing the overlap between images helps in generating more feature matches, leading to denser point clouds and more mesh faces. The GoPro Hero4 has a wide angle lens which captures a larger area per image which should lead to an increase in image overlap but it didn't seem account enough to outweigh the smaller image size.

POINT CLOUD DIFFERENCE

M3C2 takes two point cloud models as input. In this case a point cloud from the Canon 60D and a corresponding one from a GoPro Hero4. These point clouds are aligned and registered in the same coordinate system. The algorithm first computes normal vectors for each point in the point cloud models. Normals represent the direction perpendicular to the local surface at each point. M3C2 then performs a multiscale comparison by considering points at different scales or resolutions. It starts with larger scales and gradually refines the analysis to smaller scales. This approach allows for capturing both large-scale deformations and fine details in the comparison process. For each point in the reference point cloud (in this case the more dense Canon 60D point cloud was used as a reference), M3C2 searches for corresponding points in the other point cloud within a defined search radius. The search radius determines the neighborhood around each point used for comparison. The radius can be set based on the expected range of changes between the two point clouds however default settings were used. Experimentation with search radius parameters did not yield improved results for any of the cloud pairs. Once corresponding points are found, M3C2 compares the normal vectors of these points. It quantifies the differences between the normals using Euclidean distances. The magnitude of the differences indicates the discrepancy between the models at each point.

Distances were calculated for 21 paired models for nearly 310 million points. Averaging across all measured points the median distance was 6.0547mm while the mean difference was 8.8065mm. For

most modern photogrammetry applications, acceptable error ranges from 40mm to <1mm and is largely dependent on the size of the survey area (Sapirstein 2016). In underwater environments, errors as large as 1cm are accepted and present in studies which aim to measure coral growth (Rossi et al. 2020).

When viewing the distribution of distance calculation, some interesting trends emerge (Figure 10). Ubiquitous among all comparisons is white ring around the center of the model indicating no discrepancy between point clouds. Warm and cool coloration appears near the center and edges of every model. The edges of 3D models produced using photogrammetry are reconstructed on fewer reference images are more likely to exhibit artifacts and skew. Discrepancy in the edges of the point clouds appears in every model and backs up that phenomenon. Additionally, the center of the model, is saturated with color in every instance. The center of the model with respect to this study is usually a structurally complex coral colony. Discrepancies towards the middle of the model might be due to the significantly different lenses used by each platform. The GoPro Hero4 lens is a very short wide angle lens which introduces noticeable distortion towards the edges of the imagery it produces. The housing is flat lensed which doesn't introduce additional refraction. The Canon 60D lens is a standard zoom lens which doesn't distort the imagery it produces. The housing for the Canon 60D has a dome lens which can introduce a similar fish eye distortion around the edge of the frame. The strong coloration at the center of each model may be a product of the substantially different way the lenses of the two platforms interpret subject that are close to the camera.

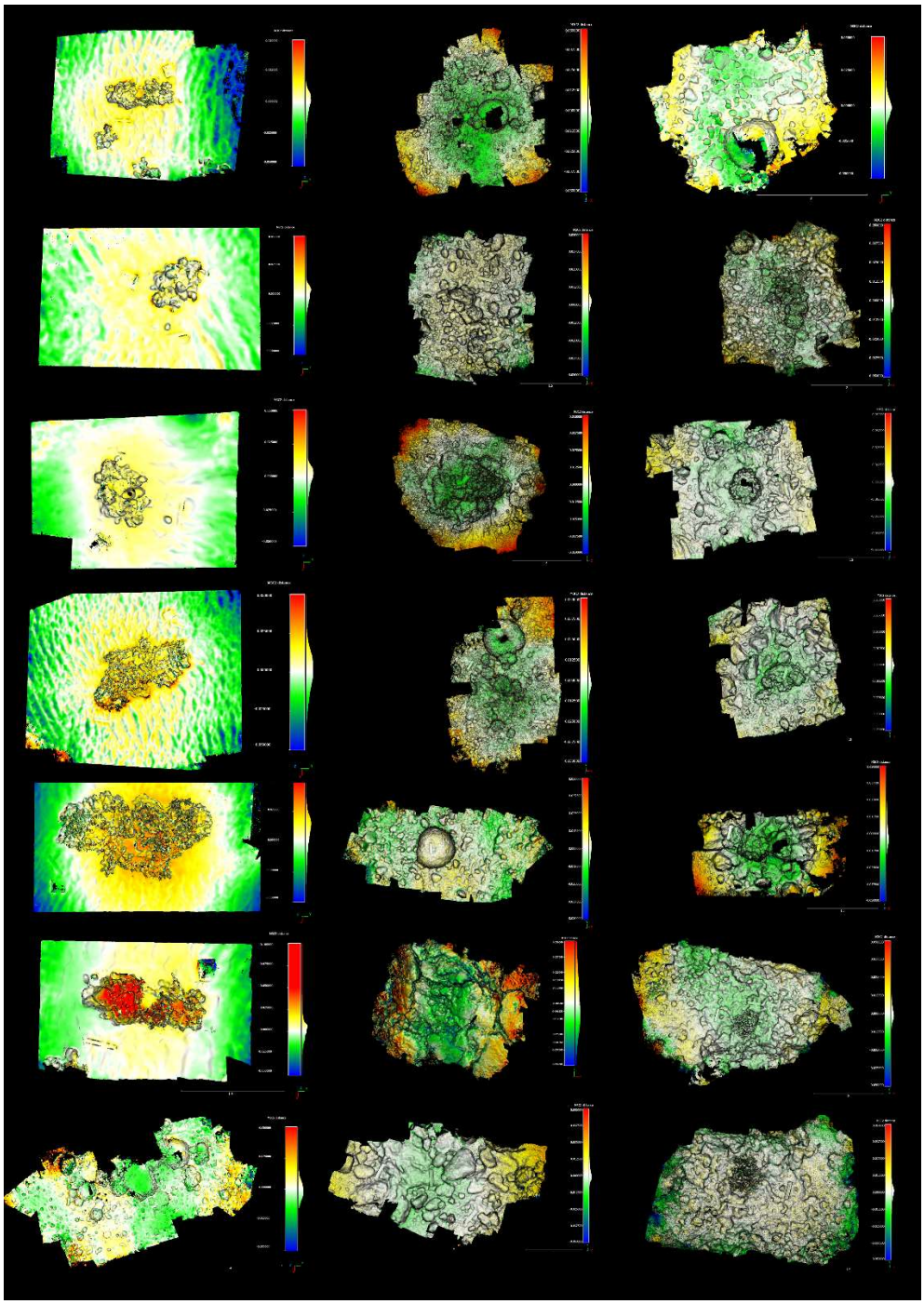

Figure 22. Illustration of M3C2 distance between point clouds collected using two camera platforms (Canon 60D and GoPro Hero4) during surveys where the camera was within 4m of the subject. Warm colors indicate areas where the GoPro Hero4 derived point cloud was further away or extended behind the Canon 60D point cloud. Cool colors indicate areas where the GoPro Hero4 point cloud was closer to observer (when viewed from above) than the Canon 60D Point cloud.

3D HABITAT STRUCTURE METRICS

All of the structural metrics generated by DEMs and 1cm/pixel and 1mm/pixel were significantly different between both the GoPro Hero4 and the Canon 60D with exception to curvature. The median slope, VRM, and surface complexity were all greater for DEMs generated by the Canon 60D compared to the GoPro Hero4. The worse quality imagery generated by the Hero4 might be artificially simplifying details in the DEMs. Curvature measures the rate of change in slope gradient and direction. As detected by the M3C2 distance comparison, both camera platforms produce reconstructions which are largely similar, but deviate at the edges and center. The structural differences detected might be related to the loss in model complexity as images lose acuity with distance. The sharp peaks and deep valleys resolved at 1m might become obscured and smoothed as both image quality and model quality drop with increased distance from the subject. While all paired DEMs were cropped to the same area, most habitat structure metrics were significantly different depending on which camera you were using.

DISTANCE FROM SUBJECT

3D model quality metrics were all significantly different across distances categories for both platforms with exception of spatial error close to the subject. Spatial error was significantly different between the cameras at the far distance. Accurately resolving the reference points on the scale bar became very difficult at 9m for the GoPro imagery. Reprojection error was significantly different across distance categories for both camera platforms. At the 6-9m distance category the difference between the two camera platforms looks like it’s breaking down. GSD was significantly different across distance categories for both camera platforms. This is not surprising as GSD is the relationship between GSD and distance is inversely proportional. As the distance between the camera sensor and the subject increases, the GSD also increases and that is reflected in Figure 21. GSD appears to exhibits a visible linear trend where the resolution decreases with increasing distance from the subject. The rate of change appears to be constant and the GSD gap between the GoPro Hero4 and Canon 60D steadily widens with an increase in distance. This resolution drop-off was especially evident when comparing two platforms at the same location 1m from the subject and 9m from the subject (Figure 23). Near to the subject, both orthomosaics resemble accurate reconstructions of the environment and the visible differences between platforms are minor. At 9m from the subject, all fine detail is lost on orthomosaic generated from the GoPro Hero4. Details on the high contrast scale bars blur together in a combination of severe chromatic aberration and poor resolution.

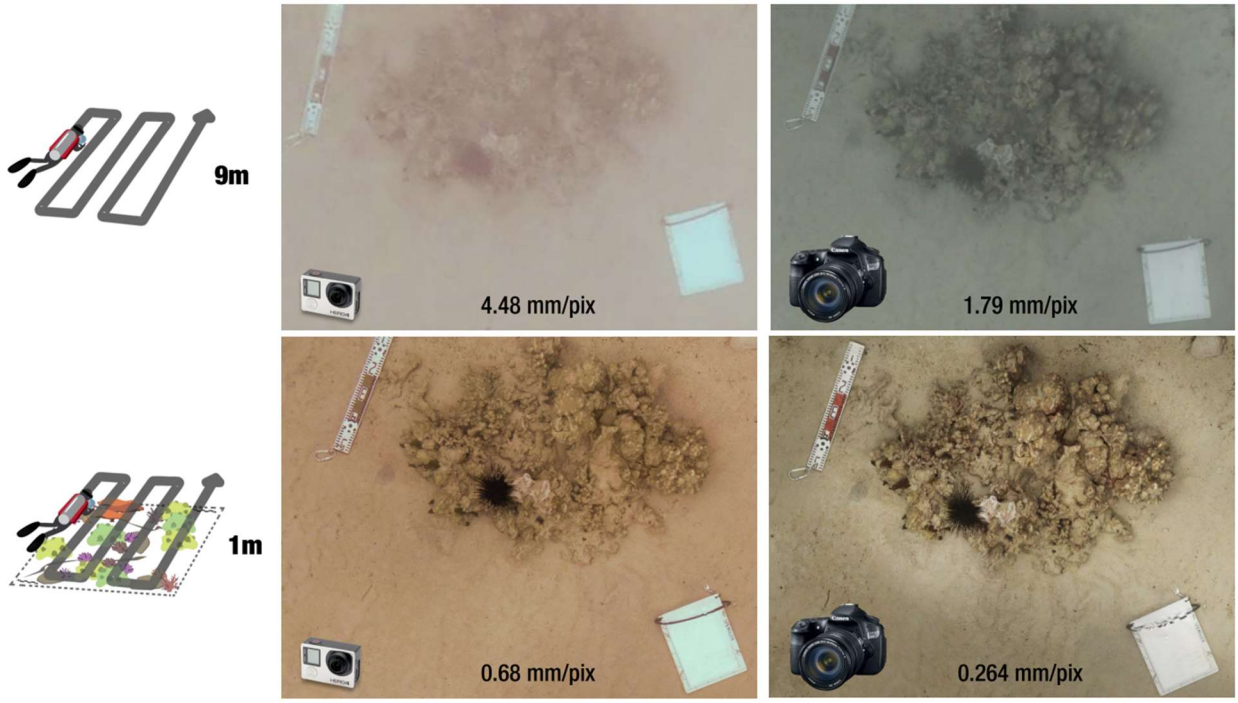

Figure 23. Comparison of the Ground Sample Distance (GSD) for orthomosaics generated from imagery captured using a GoPro Hero4 and a Canon 60D. Example imagery contrasts the furthest and nearest distances from the subject, 1 meter and 9 meters.

The three density metrics were all statistically different between the distance categories for both camera platforms. Tie point density, point cloud density, and model face density all followed a visible downward trend at the 6-9m distance. This is likely a product of the increased survey area inevitably captured by a surveyor who is collecting SfM imagery >3m from the subject. A single photo from either platform at 6m encapsulates the entire survey area. The plots for the density metrics in Figures 14, 15, and 16 show a much greater median density for the Canon 60D when it is 1-3m from the subject but a large loss in density at the 6-9m category. This might indicate that even significantly dated DSLR cameras like the Canon 60D greatly out perform simpler options like the GoPro Hero4 throughout the range densities for model characteristics.

3D habitat structure metrics exhibited a more complicated relationship with respect to distance from the subject and there were no apparent difference when the scale of the DEM was changed from the standard 1cm/pixel to 1mm/pixel. Slope was significantly different between the two camera platforms at 1-3m from the subject but that difference seems to be lost at 6-9m. VRM and surface complexity were both significantly different between the two camera platforms and two depth categories. VRM notably became much smaller as distance from the subject increased but the relationship between the two camera platforms remained the same. Curvature was not significantly different between camera platforms nor depth category.

CONCLUSION

This study aimed to assess the viability of replacing established DSLRs, such as the Canon 60D, with emerging platforms such as action cameras like the GoPro Hero4, with respect to accurate 3D reconstructions in underwater reef environments. However, the findings of this research indicate that the GoPro Hero4 falls short in several key aspects when compared to the low-end DSLRs like the Canon 60D, challenging its potential as a viable alternative.

The primary factor contributing to the superior performance of the Canon 60D is its larger sensor size and utilization of a standard lens. This combination allows the camera to capture visually rich and clearer images, which is essential for generating accurate 3D reconstructions. In contrast, the images produced by the GoPro Hero4 suffer from severe chromatic aberration and distortion, particularly towards the edges of the frame. These distortions significantly compromise the overall quality and accuracy of the resulting 3D models.

The limitations of the GoPro Hero4 further impact its viability as a replacement for low-end DSLRs. The fixed aperture and lack of exposure customization in video mode often result in overexposed images, making it challenging to capture precise and reliable data. Additionally, the GoPro Hero4's constraints in white balance customization and the absence of a reference screen hinder its ability to accurately capture colors, especially in underwater conditions where color fidelity is crucial.

Quantitative metrics further highlight the disparities between the two camera platforms. All 3D model quality metrics were significantly worse for the GoPro Hero4 when compared with the Canon 60D. However, the M3C2 algorithm, employed to compare point cloud models, revealed that point clouds generated by each platform had less than 9mm of distance discrepancy. It also brought to attention that the distribution of discrepancy is focused on the edges and center of the point clouds. Significant 3D model quality hits were found as distances increased for both camera platforms. At close distances (1-3m) both camera platforms had spatial errors which were not significantly different. All the other 3D model quality metrics were significantly different between camera platforms for the distance categories. Despite the GoPro Hero4's wider-angle lens capturing a larger area, the tiny lens and sensor adversely affected the resulting density metrics. These variations in distance calculations, influenced by lens distortion and divergent interpretations of subjects by the camera lenses, further underscore the challenges associated with action cameras as a viable replacement for low-end DSLRs.

Moreover, when evaluating how the camera systems compared with respect to 3D habitat structure metrics, curvature appeared to be the only metric unaffected by difference in the image characteristics between the platforms. Even increasing the DEM resolution from the standard 1cm/pixel to 1mm/pixel didn’t significantly change how these metrics differed between camera platform. Investigating how distance from subject affects habitat structure metrics uncovered that slope was not significantly different between the two camera platforms at 6-9m. VRM and surface complexity remained different between the two platforms for each depth category.

In conclusion, the findings of this study raise doubts regarding the feasibility of replacing low-end DSLRs like the Canon 60D with the GoPro Hero4 for accurate 3D reconstructions in underwater reef environments. The GoPro Hero4's limitations in image quality, exposure customization, color accuracy, and spatial information capture undermine its potential as a reliable alternative. Areas of research that rely on discerning fine detail should probably opt for a more higher end camera platform. Alternatively, for areas of research not beholden to fine detail, such as those interested in habitat structure metrics, small action cameras may be in line with performance of higher end platforms like DSLRs. Further research and development are needed to address these limitations and improve the performance of action cameras like the GoPro Hero4 in scientific applications. Further research utilizing more modern action cameras would likely tell a different story. While both the Canon 60D and GoPro Hero4 are significantly dated, they were able to be effectively deployed in an underwater SfM photogrammetry pipeline and produce high resolution recreations of threatened coral reef ecosystems. The inherent simplicity, convenience, low relative cost, and growing quality of small action cameras will make them an increasingly competitive option for underwater SfM photogrammetry. Their viability and potential in academia, citizen science, and beyond are evident, offering a gateway to collaborative research, community involvement, and groundbreaking scientific advancements. This democratization of technology not only fosters scientific collaboration but also cultivates a sense of environmental stewardship among individuals from diverse backgrounds. By harnessing the power of these innovative tools, we can unlock new opportunities to explore and preserve the wonders of underwater worlds, shaping a brighter future for both scientific inquiry and environmental conservation.

LITERATURE CITED

Agisoft. 2021. Agisoft Metashape User Manual version 1.8. Agisoft Metashape. Available from https://www.agisoft.com/pdf/metashape-pro_1_8_en.pdf.

Bellwood DR et al. 2019. Coral reef conservation in the Anthropocene: Confronting spatial mismatches and prioritizing functions. Biological Conservation **236**:604–615.

Burns JHR, Delparte D, Gates RD, Takabayashi M. 2015. Integrating structure-from-motion photogrammetry with geospatial software as a novel technique for quantifying 3D ecological characteristics of coral reefs. PeerJ **2015**.

Carlson BS. 2002. Evaluating image sensor sensitivity by measuring camera signal-to-noise ratio. Electro-Optical System Design, Simulation, Testing, and Training **4772**:78.

Cinner JE, McClanahan TR, Graham NAJ, Daw TM, Maina J, Stead SM, Wamukota A, Brown K, Bodin O. 2012. Vulnerability of coastal communities to key impacts of climate change on coral reef fisheries. Global Environmental Change **22**:12–20.

Dai F, Feng Y, Hough R. 2014. Photogrammetric error sources and impacts on modeling and surveying in construction engineering applications. Visualization in Engineering **2**:1–14.

DiFrancesco PM, Bonneau D, Hutchinson DJ. 2020. The implications of M3C2 projection diameter on 3D semi-automated rockfall extraction from sequential terrestrial laser scanning point clouds. Remote Sensing **12**.

Ferreira SB, Burns JHR, Pascoe KH, Clifford A. K, Reyes AJ, Fukunaga A. 2023. Prediction of habitat complexity using a trait-based approach on coral reefs in Guam. Sci Rep **13**.

Fukunaga A, Burns JHR, Craig BK, Kosaki RK. 2019. Integrating three-dimensional benthic habitat characterization techniques into ecological monitoring of coral reefs. Journal of Marine Science and Engineering 7.

Fukunaga A, Burns JHR. 2020. Metrics of coral reef structural complexity extracted from 3D mesh models and digital elevation models. Remote Sensing **12**:1–18.

Fukunaga A, Burns JHR, Pascoe KH, Kosaki RK. 2020. Associations between benthic cover and habitat complexity metrics obtained from 3D reconstruction of coral reefs at different resolutions. Remote Sensing **12**.

Graham NAJ, Nash KL. 2013. The importance of structural complexity in coral reef ecosystems. Coral Reefs **32**:315–326.

Hoegh-Guldberg, O., Mumby, P. J., Hooten, A. J., Steneck, R. S., Greenfield, P., Gomez, E., … Hatziolos ME. 2007. Change and Ocean Acidification. Science **1737**:1737–1743.

Holbrook SJ, Schmitt RJ, Messmer V, Brooks AJ, Srinivasan M, Munday PL, Jones GP. 2015. Reef fishes in biodiversity hotspots are at greatest risk from loss of coral species. PLoS ONE **10**:1–12.

Hughes TP. 2003. Climate Change, Human Impacts, and the Resilience of Coral Reefs. Science **301**:929–933.

Lague D, Brodu N, Leroux J. 2013. Accurate 3D comparison of complex topography with terrestrial laser scanner: Application to the Rangitikei canyon (N-Z). ISPRS Journal of Photogrammetry and Remote Sensing **82**:10–26.

Lecours V, Devillers R, Simms AE, Lucieer VL, Brown CJ. 2017. Towards a framework for terrain attribute selection in environmental studies. Environmental Modelling and Software **89**:19–30. Elsevier Ltd. Available from http://dx.doi.org/10.1016/j.envsoft.2016.11.027.

Licuanan WY, Mordeno PZB, Go M V. 2021. C30 — A simple, rapid, scientifically valid, and low-cost method for citizen-scientists to monitor coral reefs. Regional Studies in Marine Science **47**:101961. Elsevier B.V. Available from https://doi.org/10.1016/j.rsma.2021.101961.

Menna F, Nocerino E, Drap P, Remondino F, Murtiyoso A, Grussenmeyer P, Börlin N. 2018. Improving underwater accuracy by empirical weighting of image observations. International Archives of the Photogrammetry, Remote Sensing and Spatial Information Sciences - ISPRS Archives **42**:699–705.

Nocerino E, Neyer F, Gruen A, Troyer M, Menna F, Brooks A, Capra A, Castagnetti C, Rossi P. 2019. Comparison Of Diver-Operated Underwater Photogrammetric Systems For Coral Reef Monitoring. ISPRS Annals of the Photogrammetry, Remote Sensing and Spatial Information Sciences **42**:143–150.

O'Connor J. 2018. Impact of image quality on SfM Photogrammetry : colour , compression and noise (PhD thesis). Undefined. Available from https://ethos.bl.uk/OrderDetails.do?uin=uk.bl.ethos.789344.

Raoult V, David PA, Dupont SF, Mathewson CP, O'Neill SJ, Powell NN, Williamson JE. 2016. GoProsTM as an underwater photogrammetry tool for citizen science. PeerJ **2016**.

Reaka-Kudla, M.L. 1997. The global biodiversity of coral reefs: a comparison with rain forests. Biodiversity II: Understanding and protecting our biological resources **2**:551.

Risk MJ. 1972. Fish Diversity on a Coral Reef in the Virgin Islands. Atoll Research Bulletin **153**:1–4. Available from https://repository.si.edu/bitstream/handle/10088/6067/00153.pdf.

Roach TNF et al. 2021. A field primer for monitoring benthic ecosystems using structure-from-motion photogrammetry. Journal of Visualized Experiments **2021**:1–14.

Roberts CJ, Vergés A, Callaghan CT, Poore AGB. 2022. Many cameras make light work: opportunistic photographs of rare species in iNaturalist complement structured surveys of reef fish to better understand species richness. Biodiversity and Conservation **31**:1407–1425.

Rossi P, Castagnetti C, Capra A, Brooks AJ, Mancini F. 2020. Detecting change in coral reef 3D structure using underwater photogrammetry: critical issues and performance metrics. Applied Geomatics **12**:3–17. Applied Geomatics.

Sapirstein P. 2016. Accurate measurement with photogrammetry at large sites. Journal of Archaeological Science **66**:137–145. Elsevier Ltd. Available from http://dx.doi.org/10.1016/j.jas.2016.01.002.

Tebbett SB, Streit RP, Bellwood DR. 2020. A 3D perspective on sediment accumulation in algal turfs: Implications of coral reef flattening. Journal of Ecology **108**:70–80.

Wilkinson C, Souter D. 2008. Status of Caribbean coral reefs after bleaching and hurricanes in 2005.Global Coral Reef Monitoring Network, and Reef and Rainforest Research Centre, Townsville, 152 p.

Young GC, Dey S, Rogers AD, Exton D. 2017. Cost and time-effective method for multiscale measures of rugosity, fractal dimension, and vector dispersion from coral reef 3D models. PLoS ONE **12**:1–18.

CHAPTER 2
Immersive Exploration of Pacific Coral Reefs and Wrecks: An Augmented Reality Application Leveraging Structure from Motion Photogrammetry

INTRODUCTION

The Earth's oceans are home to an extraordinary array of biodiversity and include diverse ecosystems that are crucial for the planet's health and resilience (Komyakova, Munday, & Jones 2013). Coral reefs serve as foundational ecosystems and critical hotspots of biodiversity (Hughes, Bellwood, & Connolly 2002). The complex structures created by corals provide a foundation for the reef, offering habitats through their 3D structural complexity (Graham & Nash 2013). These structures also provide vital ecosystem services, such as shoreline protection, nutrient cycling, and carbon sequestration (Moberg & Folke 1999). Moreover, coral reefs are cultural treasures, deeply intertwined with indigenous communities who have relied on them for sustenance, livelihoods, and cultural practices for centuries (Grafeld et al. 2017).

In addition to coral reefs, the Pacific Ocean is home to numerous shipwrecks that serve as poignant reminders of historical events, particularly those related to World War II. Guam, an island in the western Pacific, witnessed intense military operations during the war, leaving behind a legacy of sunken vehicles from naval battles. These wrecks, now submerged beneath the waves, hold both historical and archaeological significance, representing tangible links to the past.

The exploration and study of these submerged environments have long been confined to a privileged few - a select group of marine scientists and divers equipped with specialized training and equipment. The remote locations, extreme depths, and challenging diving conditions have limited access to these environments. Consequently, exploration and appreciation of these underwater ecosystems and historical wrecks remains out of reach for many. To bridge this knowledge gap and democratize access to these hidden treasures, technological advancements in structure from motion (SfM) photogrammetry and augmented reality (AR) offer transformative solutions.

SfM photogrammetry is a powerful data collection method used to reconstruct accurate 3D models from a collection of 2D photographs. In this project we leverage underwater SfM photogrammetry assets that have been actively used in scientific research, ensuring the accuracy and authenticity of the resulting models. These assets are derived from high-resolution underwater photographs captured by divers on SCUBA during dedicated marine expeditions. The photogrammetric reconstruction process extracts dense point clouds and high-resolution textures, preserving the intricate details of the coral reefs and wrecks in sub centimeter resolution (Burns & Delparte 2017).

The Unity game engine provides the necessary tools and infrastructure to develop the AR application, facilitating the integration of the SfM-based 3D models into a user-friendly and interactive interface. The Vuforia AR engine augments reality by enabling real-time tracking of the physical environment, superimposing the virtual models onto the user's real-world surroundings. The combination of these technologies offers a seamless and captivating experience, allowing users to freely navigate and explore the virtual underwater landscapes and objects, while still maintaining a connection to the real world. By utilizing Unity, an interactive game engine, and the Vuforia AR engine, we have developed an

innovative AR application that allows users to virtually explore and observe underwater models of coral reefs and wrecks from the Pacific region. These models, generated through SfM photogrammetry using actively utilized assets, enable a visually stunning and immersive experience, overcoming the limitations of physical access and providing a platform for education, research, and conservation efforts.

Furthermore, the AR application goes beyond mere visualization, incorporating educational and informative elements to enhance the user experience. Interactive annotations, informative overlays, and engaging multimedia content provide valuable insights into the ecological dynamics of coral reefs, the historical context of shipwrecks, and ongoing scientific research and conservation efforts. This integration of educational content with immersive AR technology holds great potential in fostering environmental awareness, promoting interdisciplinary research collaboration, and facilitating public engagement in marine sciences and cultural heritage preservation.

The primary objective of this study is to introduce and evaluate the effectiveness of an AR application in providing an immersive and educational experience to users, while also showcasing the practical application of SfM photogrammetry assets actively used in scientific research. By leveraging the power of Unity and Vuforia, combined with the wealth of data generated from underwater SfM photogrammetry, we created a seamless integration of virtual underwater environments into the real world, providing users with an unprecedented opportunity to explore and learn about Pacific coral reefs and wrecks. By providing users with an immersive and educational experience, the application not only enables virtual access to these captivating underwater environments but also contributes to the broader goals of environmental conservation, scientific research, and cultural heritage appreciation.

METHODS

DATA ACQUISITION AND SFM PHOTOGRAMMETRY

High-resolution underwater photographs were captured using scuba divers' cameras during SfM photogrammetry surveys on dedicated marine expeditions across various locations in the Pacific Ocean. Locations included Apra Harbor in Guam, Lalo in the Papahānaumokuākea Marine National Monument, Honolulu in Oahu, and Hilo Hawaii. Models were rendered in Agisoft Metashape (Metashape v.1.7.1) following techniques created specifically for 3D reconstructions from coral reef habitats as described in Burns et al. (2015). The pipeline included image alignment, dense point cloud generation, mesh reconstruction, and texture mapping. In order to minimize file size and asset loading times, high resolution 3D models were decimated (typically face counts were reduced down to 400,000 faces) and rendered with a slightly smaller texture size (10,000 x 10,000 pixels). This was done with the goal of reducing total model size (model and texture) to roughly 100MB. Models were also cropped to rectangular dimensions for a more clean appearance while augmented (Figure 24). Final models were exported as .OBJ and textures as .JPG for use in Unity. 9 high resolution 3D models were included in the app as of May 30th 2023. Augmented reality video playback functionality was added after release and consisted of videos cut down to <30 seconds, reduced to 1080p, and converted to .mp4 format. This was also done to reduce total app size and prevent issues with playback. 13 videos were created for the app as of May 30th 2023.

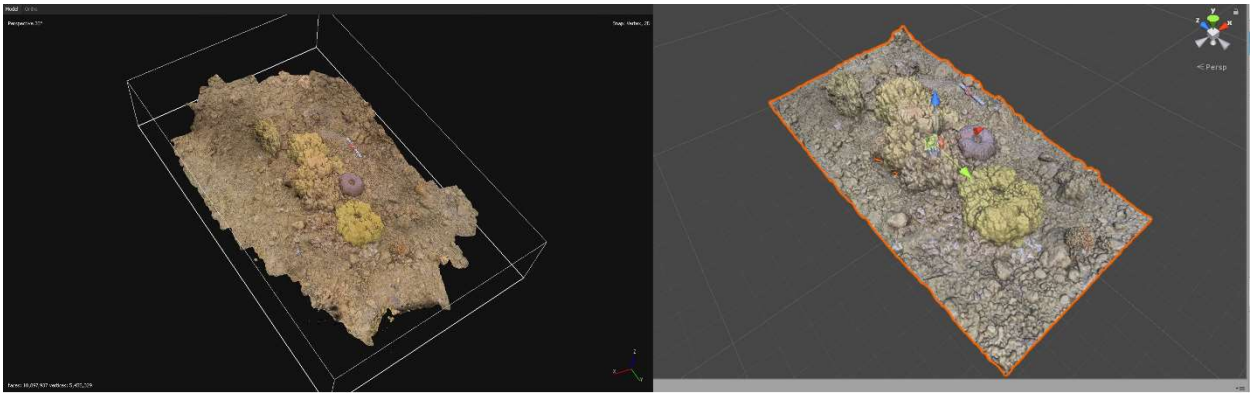

Figure 24. Preparation of 3D model produced through underwater SfM photogrammetry. 3D model in Agisoft Metashape before decimation, texture reduction, and cropping. File size = 850MB (Left). 3D model in Unity after decimation, texture reduction, and cropping. File size = 103MB (Right).

APPLICATION DEVELOPMENT

The application was primarily developed in Unity (Unity version 2018.4.20f1). Seven scenes were created, each experienced as a difference screen. This included the splash warning screen (required on publicly available AR apps), tutorial screens, main menu screen, main application screen, and an about screen. The application's user interface (UI) was designed to provide an intuitive and immersive experience. With this in mind, the app was developed with a full spectrum of modern screen sizes in mind, ranging from small phones to large tablets. UI objects such as buttons, text, and imagery were anchored to specific regions of the screen. Many of the text and images are set to scale within bounds to the devices screen size. The app opens with a mandated warning and then enters into a skippable visual tutorial (Figure 25). A tutorial menu was included as some of the concepts related to augmented reality and 3D models can be difficult to intuit from the perspective of a broad audience. Tutorial graphics and buttons throughout the app were created in Adobe Photoshop (version 24.0.0) and Illustrator (version 27.0). Navigation between menus and interactions with UI elements such as info boxes were scripted in C#. An “information” button labeled with an “i” was included and on interaction triggered a popup menu. This popup menu includes site specific information as well as a map which corresponds to the model (Figure 26).

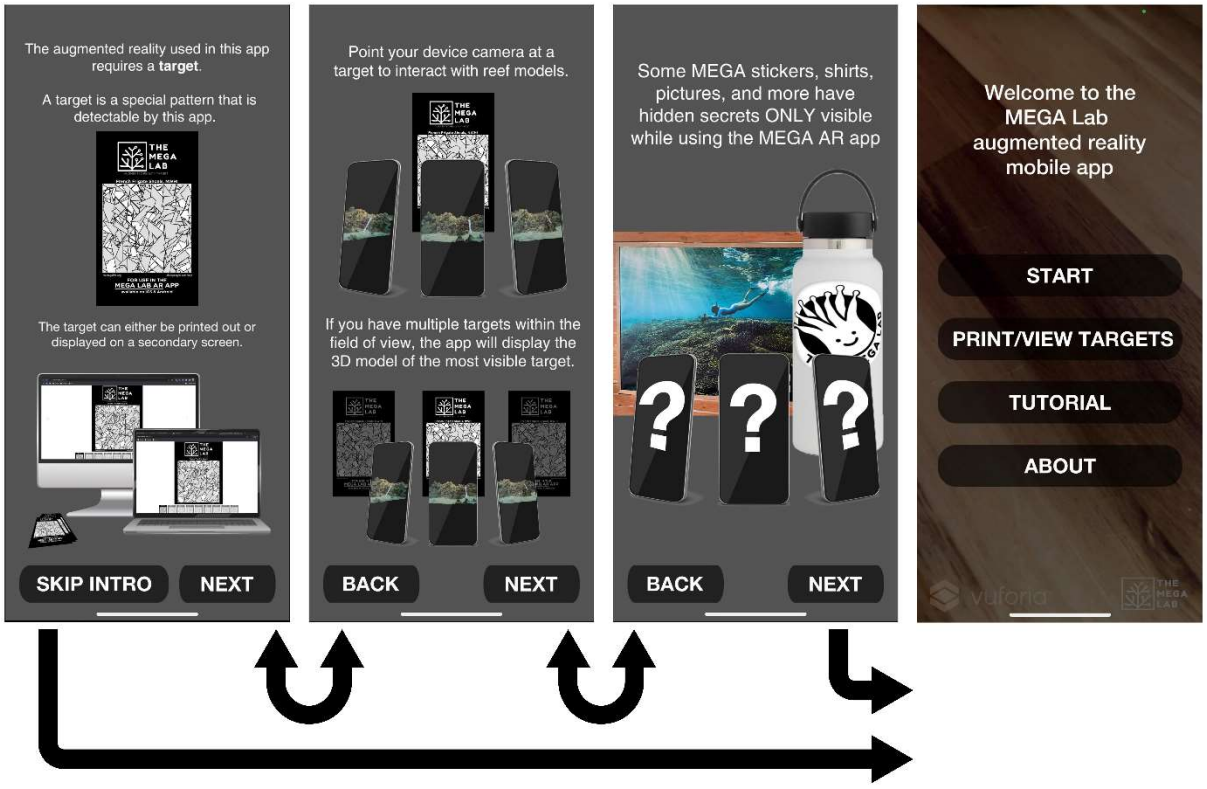

Figure 25. Screenshots of the visual tutorial played at start of the application. Tutorial depicts how to use this target based augmented reality app. The main menu is visualized on the far right.

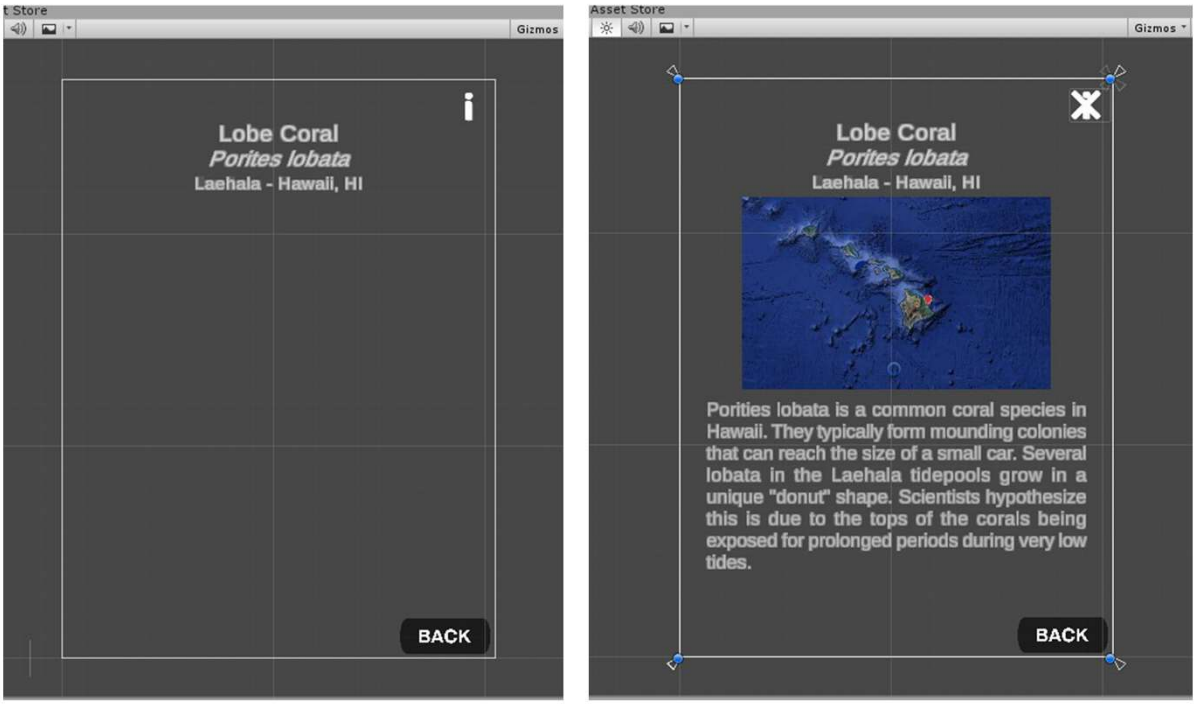

Figure 26. Development view of the main app UI in Unity illustrating model name, location, as well as the interactive information button on the top right (left). On pressing the “I” a corresponding information popup appears (right).

The Vuforia Engine (Vuforia version 10.15.4) was used as the platform for advanced computer vision functionality throughout this app. The simplest method of augmentation is to use image targets that the Vuforia Engine can detect and track. A simple random pattern consisting of grey triangles and lines was created in Adobe Illustrator. Nine of these patterns were generated and uploaded to Vuforia’s Target Manger. This pattern was validated and given the highest performance rating for detectability and tracking in the Vuforia Engine. A target database was generated by Vuforia, downloaded, and imported into Unity. This allowed for the association between target and corresponding model in Unity. 3D models were appropriately scaled to correspond with real world target size and digitally superimposed on the target (Figure 27). On target detection, the associated object was scripted to be rendered. In order limit computational stress, target tracking was limited to a single target. After the application was released, 19 more targets were added to the app. These were associated with real world stickers, logos, and imagery produced by the MEGA Lab. For each of these targets, a VideoPlayer object was attached to a 2D plane which was superimposed over the target (Figure 28). On target detection, the VideoPlayer was scripted to begin playing an associated video. On target loss the VideoPlayer was scripted to pause. This allowed a user to continue watching a video without having to restart every time.

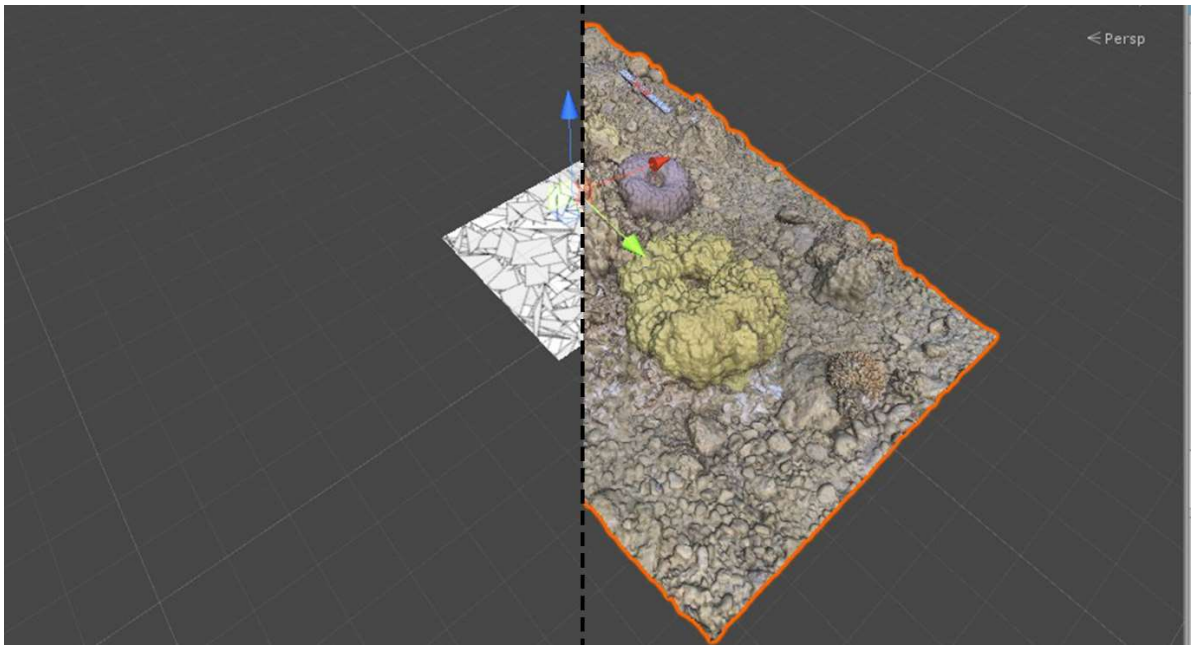

Figure 27. Development view in Unity with a illustrated cutaway showing the augmented reality target beneath the 3D model. This is how large the 3D model would be augmented upon a real world target.

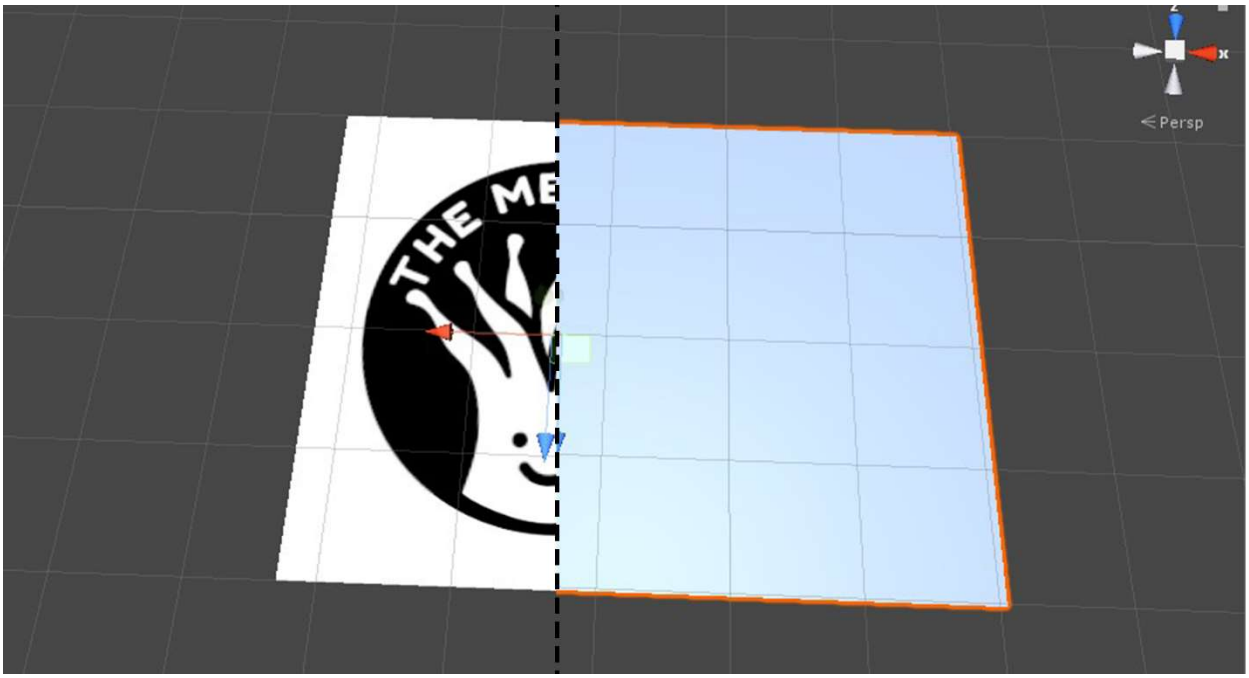

Figure 28. Development view in Unity with a illustrated cutaway showing the augmented reality target beneath the VideoPlayer plane. This is how large the video would be augmented upon a real world target.

Prior to publication, a group of 17 participants, including marine scientists, divers, and members of the general public, were recruited to evaluate the usability and effectiveness of the AR application. The performance of the AR application, including rendering speed, tracking accuracy, and resource utilization, was assessed on various mobile devices. Benchmarking tests were conducted to measure frame rates, latency, and power consumption, ensuring optimal performance across different hardware specifications. Their feedback and recommendations were incorporated into the refinement of the application.

PUBLISHING

Both Android and iOS versions of the app were exported from Unity and compiled using Microsoft Visual Studio 2022 (version 17.6). The iOS version was exported from Unity and Microsoft Visual Studio into Xcode (version 14). The app was further complied for iOS platforms, optimized, signed with an Apple Developer key, and uploaded to App Store Connect for review. After review the application was publicly available for download. The Android version of the app was exported from Unity using the native integration with Android Software Development Kit (SDK) and the Google Android App bundle extension for packaging large applications. Optimization and signing for the Android version of the app was accomplished in Unity, then uploaded to the Google Play Console for review. As of May 30th 2023 the Android app does not contain the video assets but development is ongoing.

RESULTS

MEGA Lab AR was initially released on April 13th 2020 for Android devices on the Google Play store and Aug 2nd 2020 for iOS devices on the Apple App Store. As of May 31st 2023, the iOS app has been downloaded 1,531 times and has a 5 star rating on the app store. The Android version has been downloaded 148 times on the Google Play Store. The iOS app has 20,158 impressions on the Apple App Store. The Android app has 652 impressions on the Google Play Store. There have been 7 major iOS updates and 6 major android updates. The iOS version is 1.4GB and includes 9 high resolution models and 13 short 1080p videos. The Android version is 122MB but contains older models and no videos. The MEGA Lab AR app is currently a primary outreach tool for the MEGA Lab has been implemented at most public facing events across all age ranges since its release. Video target functionality was added in December 2022. Additional videos were added in January 2023 to support the contemporary art project titled He‘e Nalu: The Art and Legacy of Hawai‘ian Surfing (2023) at the Heard Museum in Phoenix Arizona. In February 2023 the app was featured in a monthlong event in the exhibit “He Honua Ola: A Thriving Coral Reef” at ‘Imiloa Astronomy Center in Hilo Hawai‘i (Figure 29).

Figure 29. Real world outreach applications of the MEGA Lab AR app. App being used alongside the He Honua Ola: A Thriving Coral Reef” exhibit at the ‘Imiloa Astronomy Center in Hilo Hawaii (far left). Other images from various educational outreach events.

DISCUSSION

The development and implementation of the MEGA Lab AR app has successfully bridged the gap between scientific data products derived from underwater SfM photogrammetry and the general public. This intuitive app allows users, including children, to explore and interact with 3D models and videos by simply pointing their smart devices at designated targets. The app's user-friendly interface and immersive experience have proven effective in engaging users of all ages, opening up new possibilities for educational outreach initiatives. One notable outcome of the app's deployment is its ability to inspire and facilitate student engagement. By encouraging students to create their own 3D models using photogrammetry and subsequently experiencing them in augmented reality, the app fosters a deeper understanding and connection with physical objects transformed into digital representations. This experiential learning approach surpasses the limitations of traditional instructional methods, effectively communicating complex concepts and ideas. Expanding the target library to include logos and images has greatly expanded the app's potential for engagement. This enhancement allows for the inclusion of numerous 3D objects or videos, transforming seemingly ordinary spaces into interactive and dynamic experiences. The addition of video targets further diversifies the app's content, catering to users who prefer a more passive consumption of information. This versatility broadens the app's appeal and potential for widespread use.

However, it is worth noting that the app currently struggles to maintain users' attention over extended periods. While the initial excitement and fascination are evident, some users tend to exhaust all available targets relatively quickly, resulting in a decrease in engagement. This observation presents an opportunity for future iterations of the app to incorporate a larger number of targets, pulling from a broader range of 3D models and videos accessible through an internet connection. Improvements in the app could allow for a user to download packages related to famous surf breaks, historic wrecks, or facilitate the identification of coral species and disease. This approach would enrich the user experience and provide a continuously expanding array of content.

One significant challenge faced by the app is its large file size, currently standing at 1.4GB. This poses several issues, including the need for ample storage space, a fast data connection, and user patience during the initial download. The size limitation has also hindered app adoption, particularly in settings with limited internet access, such as the collaboration with the Heard Museum in Phoenix, Arizona, and ʻImiloa Astronomy Center in Hilo, Hawaiʻi. To overcome this challenge and improve user accessibility, future iterations should focus on optimizing the app's size by offering a smaller base app with the option to download additional content packages, tailored to specific user interests. This approach would alleviate storage concerns and allow for the inclusion of more models and content without breaching app store limits. At first release, the MEGA Lab AR app it was much smaller (around 120MB). Like all Android apps of the time, the Android version of MEGA Lab AR was exported as an Android Application Pack (APK). This was the typical distribution file for Android apps since its inception. In

August 2021 Google permanently switched to only supporting the new Android App Bundle (AAB) distribution type. This necessitates a slight rebuild of the Android version of the MEGA Lab AR app before it can be accepted by the Google Play Store. Both the Android and iOS versions of the app are built in an outdated version of Unity. Rebuilding the app may also alleviate strange bugs like intermittent video and audio playback issues on some devices.

Exploration of alternative augmented reality techniques, such as Simultaneous Localization and Mapping (SLAM), holds promise for future app development. Moving away from target-based AR, SLAM-based AR could offer a more streamlined user experience, eliminating the need for specific image targets. A potential avenue for further development would involve creating a comprehensive app that guides users through the process of collecting their own SfM photogrammetry data, processing it in the cloud, and enabling viewing without the reliance on targets. This approach could transform the app into a powerful citizen science tool, encouraging users to contribute to marine research efforts by collecting geolocated imagery and sharing it with professionals worldwide. The MEGA Lab AR app has successfully brought underwater SfM photogrammetry data to a wider audience, providing an immersive and educational experience. However, further improvements are necessary to enhance long-term user engagement, optimize app size for broader accessibility, and explore innovative techniques like SLAM-based AR. By addressing these challenges and expanding the app's capabilities, we can unlock the full potential of augmented reality as a tool for marine science education, citizen science, and outreach initiatives.

CONCLUSION

In conclusion, the development and release of our AR application have successfully merged the realms of technology, scientific research, and public outreach. By leveraging Unity, Vuforia, and assets from underwater SfM photogrammetry actively used in scientific projects, we have created an immersive and educational platform for users to explore and appreciate the beauty and significance of Pacific coral reefs and historical shipwrecks. However, the app's current limitations in sustaining long-term engagement and its substantial file size pose challenges. To address these challenges, future iterations should focus on expanding the target library, incorporating a wider range of 3D models and videos accessible through internet connectivity. Moreover, optimizing the app's size by providing a smaller base version with downloadable content packages would alleviate storage concerns and improve user adoption. Additionally, exploring alternative augmented reality techniques, such as SLAM-based AR, shows promise for enhancing the app's capabilities and eliminating reliance on specific image targets. By addressing these aspects, the MEGA Lab AR app has the potential to become a powerful educational and citizen science tool, enabling users to actively contribute geolocated imagery for marine research and promoting engagement in marine science outreach. This app bridges the gap between scientific data and the public, revolutionizing the way we interact with marine environments and fostering global participation in marine research endeavors. Through this application, we strive to foster environmental stewardship, promote interdisciplinary collaboration, and inspire a deeper understanding of our oceans and their fragile ecosystems

LITERATURE CITED

Agisoft. 2021. Agisoft Metashape User Manual version 1.7. Agisoft Metashape. Available from https://www.agisoft.com/pdf/metashape-pro_1_7_en.pdf.

Apple Xcode 14. Available online https://developer.apple.com/xcode/ (accessed on 30 May 2023).

Burns JHR, Delparte D, Gates RD, Takabayashi M. 2015. Integrating structure-from-motion photogrammetry with geospatial software as a novel technique for quantifying 3D ecological characteristics of coral reefs. PeerJ **2015**.

Burns JHR, Delparte D. 2017. Comparison of commercial structure-from-motion photogrammety software used for underwater three-dimensional modeling of coral reef environments. International Archives of the Photogrammetry, Remote Sensing and Spatial Information Sciences - ISPRS Archives **42**:127–131.

Grafeld S, Oleson KLL, Teneva L, Kittinger JN. 2017. Follow that fish: Uncovering the hidden blue economy in coral reef fisheries. PLoS ONE **12**:1–25.

Graham NAJ, Nash KL. 2013. The importance of structural complexity in coral reef ecosystems. Coral Reefs **32**:315–326.

Hughes TP, Bellwood DR, Connolly SR. 2002. Biodiversity hotspots, centres of endemicity, and the conservation of coral reefs. Ecology Letters **5**:775–784.

Komyakova V, Munday PL, Jones GP. 2013. Relative importance of coral cover, habitat complexity and diversity in determining the structure of reef fish communities. PLoS ONE **8**:1–12.

Microsoft Android Studio | Android Developers. Available online: https://developer.android.com/studio (accessed on 30 May 2023)

Moberg F, Folke C. 1999. Ecological goods and services of coral reef ecosystems. Ecological Economics **29**:215–233.

Unity Technologies Real-Time Solutions. Endless Opportunities. Available online: https://unity.com/ (accessed on 30 May 2023).

Vuforia Vuforia Engine. Available online: https://developer.vuforia.com/ (accessed on 30 May 2023).